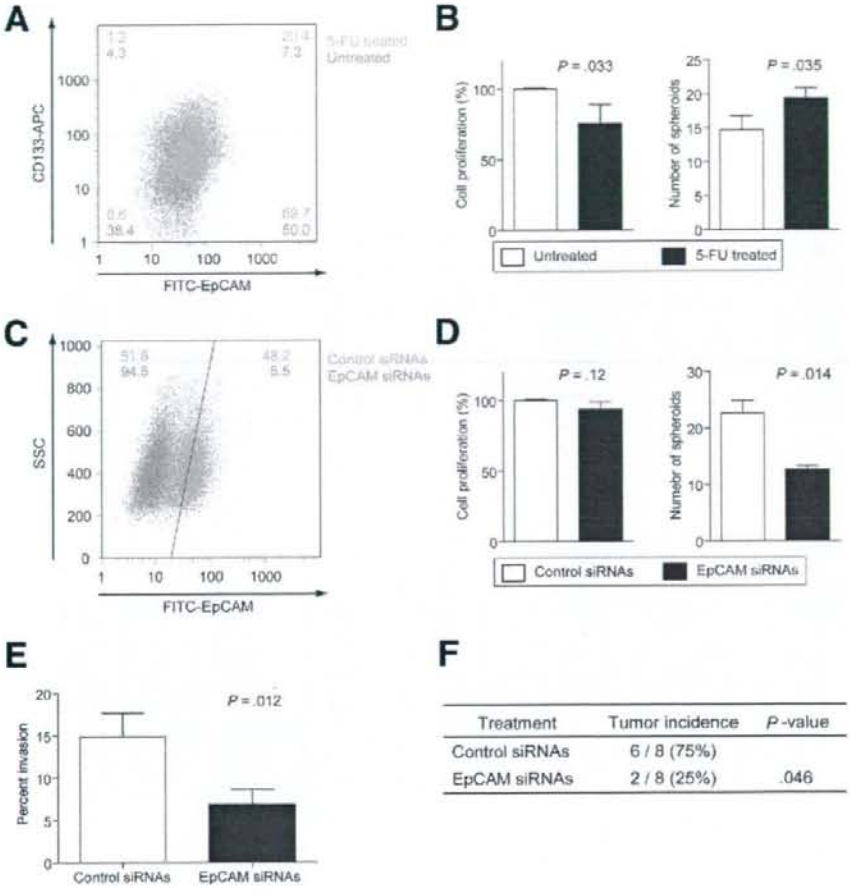

F

Treatment	Tumor incidence	*P*-value
Control siRNAs	6 / 8 (75%)	
EpCAM siRNAs	2 / 8 (25%)	.046

Figure 7. EpCAM blockage inhibits the tumorigenic and invasive capacity of EpCAM$^+$ HCC cells. (*A*) Enrichment of EpCAM$^+$ cells after 5-FU treatment. HuH1 cells refer as control or without treatment (*green*) or treated with 2 μg/mL of 5-FU (*orange*) for 3 days and analyzed by FACS using anti-EpCAM and anti-CD133 antibodies. (*B*) Spheroid formation of HuH1 cells treated with 2 μg/mL of 5-FU for 3 days. (*C*) FACS analysis of HuH1 cells treated with a control siRNA (orange) or EpCAM-specific siRNA (*green*) at day 3 after transfection. (*D*) Spheroid formation or (*E*) invasive capacity ofEpCAM$^+$ HuH1 cells transfected with a control siRNA or EpCAM-specific siRNA. Experiments were performed in triplicate and the data are shown as mean ± SD. (*D*) siRNAs. (*F*) Inhibition of tumor formation in vivo by EpCAM gene silencing. EpCAM$^+$ HuH1 cells were transfected with siRNA oligos and 1000 cells were injected 24 hours after transfection.

comprehensively investigate the expression patterns of stem cell markers to characterize the population of CSCs that may correlate with the activation of their distinct molecular pathways.

CSCs may be more resistant to chemotherapeutic agents than differentiated tumor cells possibly owing to an increased expression of adenosine triphosphate–binding cassette transporters and anti-apoptotic proteins.[4] Thus, the development of an effective strategy to target CSC pools together with conventional chemotherapies is essential to eradicate a tumor mass.[14] By blocking the programs that activate self-renewal and/or inhibit asymmetric division, CSC features could be destemmed.[46,47] Consistently, EpCAM blockage could inhibit cellular invasion and tumorigenicity of EpCAM$^+$ HCC cells, revealing the feasibility of targeting a CSC marker to destem CSC features. EpCAM may induce c-Myc,[48] a common molecular node activated in HpSC-HCC.[27] c-Myc, together with Oct3/4, Sox2, and Klf4, can induce pluripotent stem cells from adult fibroblasts.[49] It is possible that EpCAM blockage to inhibit hepatic CSCs may result in a suppression of c-Myc signaling. Encouragingly, EpCAM-specific antibodies are currently in phase II clinical trials.[50] Furthermore, a recent study indicated that EpCAM$^+$ circulating tumor cells identified by a unique microfluidic platform can be used to monitor outcomes of patients undergoing systemic treatment.[51] Therefore, it may be useful to combine EpCAM antibodies with conventional chemotherapy to target both CSCs and non-CSCs for the treatment of HCC.

Supplementary Data

Note: To access the supplementary material accompanying this article, visit the online version of *Gastroenterology* at www.gastrojournal.org, and at doi: 10.1053/j.gastro.2008.12.004.

References

1. Fialkow PJ. Clonal origin of human tumors. Biochim Biophys Acta 1976;458:283–321.

2. Heppner GH. Tumor heterogeneity. Cancer Res 1984;44:2259–2265.
3. Hanahan D, Weinberg RA. The hallmarks of cancer. Cell 2000;100:57–70.
4. Jordan CT, Guzman ML, Noble M. Cancer stem cells. N Engl J Med 2006;355:1253–1261.
5. Clarke MF, Dick JE, Dirks PB, et al. Cancer stem cells—perspectives on current status and future directions: AACR Workshop on cancer stem cells. Cancer Res 2006;66:9339–9344.
6. Potter VR. Phenotypic diversity in experimental hepatomas: the concept of partially blocked ontogeny. The 10th Walter Hubert Lecture. Br J Cancer 1978;38:1–23.
7. Sell S. Cellular origin of cancer: dedifferentiation or stem cell maturation arrest? Environ Health Perspect 1993;101(Suppl 5):15–26.
8. Wicha MS, Liu S, Dontu G. Cancer stem cells: an old idea—a paradigm shift. Cancer Res 2006;66:1883–1890.
9. Al Hajj M, Wicha MS, Benito-Hernandez A, et al. Prospective identification of tumorigenic breast cancer cells. Proc Natl Acad Sci U S A 2003;100:3983–3988.
10. Singh SK, Hawkins C, Clarke ID, et al. Identification of human brain tumour initiating cells. Nature 2004;432:396–401.
11. Bonnet D, Dick JE. Human acute myeloid leukemia is organized as a hierarchy that originates from a primitive hematopoietic cell. Nat Med 1997;3:730–737.
12. Ricci-Vitiani L, Lombardi DG, Pilozzi E, et al. Identification and expansion of human colon-cancer-initiating cells. Nature 2007;445:111–115.
13. O'Brien CA, Pollett A, Gallinger S, et al. A human colon cancer cell capable of initiating tumour growth in immunodeficient mice. Nature 2007;445:106–110.
14. Dean M, Fojo T, Bates S. Tumour stem cells and drug resistance. Nat Rev Cancer 2005;5:275–284.
15. Rich JN. Cancer stem cells in radiation resistance. Cancer Res 2007;67:8980–8984.
16. Parkin DM, Bray F, Ferlay J, et al. Global cancer statistics, 2002. CA Cancer J Clin 2005;55:74–108.
17. Sell S, Pierce GB. Maturation arrest of stem cell differentiation is a common pathway for the cellular origin of teratocarcinomas and epithelial cancers. Lab Invest 1994;70:6–22.
18. Thorgeirsson SS, Grisham JW. Hepatic stem cells. Semin Liver Dis 2003;23:301.
19. Thorgeirsson SS, Grisham JW. Molecular pathogenesis of human hepatocellular carcinoma. Nat Genet 2002;31:339–346.
20. Lee JS, Heo J, Libbrecht L, et al. A novel prognostic subtype of human hepatocellular carcinoma derived from hepatic progenitor cells. Nat Med 2006;12:410–416.
21. Sigal SH, Brill S, Fiorino AS, et al. The liver as a stem cell and lineage system. Am J Physiol 1992;263:G139–G148.
22. Schmelzer E, Wauthier E, Reid LM. The phenotypes of pluripotent human hepatic progenitors. Stem Cells 2006;24:1852–1858.
23. Schmelzer E, Zhang L, Bruce A, et al. Human hepatic stem cells from fetal and postnatal donors. J Exp Med 2007;204:1973–1987.
24. Dan YY, Riehle KJ, Lazaro C, et al. Isolation of multipotent progenitor cells from human fetal liver capable of differentiating into liver and mesenchymal lineages. Proc Natl Acad Sci U S A 2006;103:9912–9917.
25. Zaret KS. Regulatory phases of early liver development: paradigms of organogenesis. Nat Rev Genet 2002;3:499–512.
26. Shafritz DA, Oertel M, Menthena A, et al. Liver stem cells and prospects for liver reconstitution by transplanted cells. Hepatology 2006;43:S89–S98.
27. Yamashita T, Forgues M, Wang W, et al. EpCAM and alpha-fetoprotein expression defines novel prognostic subtypes of hepatocellular carcinoma. Cancer Res 2008;68:1451–1461.
28. Reya T, Clevers H. Wnt signalling in stem cells and cancer. Nature 2005;434:843–850.
29. Yamashita T, Budhu A, Forgues M, et al. Activation of hepatic stem cell marker EpCAM by Wnt-β-catenin signaling in hepatocellular carcinoma. Cancer Res 2007;67:10831–10839.
30. Budhu A, Forgues M, Ye QH, et al. Prediction of venous metastases, recurrence and prognosis in hepatocellular carcinoma based on a unique immune response signature of the liver microenvironment. Cancer Cell 2006;10:99–111.
31. Ye QH, Qin LX, Forgues M, et al. Predicting hepatitis B virus-positive metastatic hepatocellular carcinomas using gene expression profiling and supervised machine learning. Nat Med 2003;9:416–423.
32. Wu CG, Forgues M, Siddique S, et al. SAGE transcript profiles of normal primary human hepatocytes expressing oncogenic hepatitis B virus X protein. FASEB J 2002;16:1665–1667.
33. Kubota H, Reid LM. Clonogenic hepatoblasts, common precursors for hepatocytic and biliary lineages, are lacking classical major histocompatibility complex class I antigen. Proc Natl Acad Sci U S A 2000;97:12132–12137.
34. Yoshikawa H, Matsubara K, Zhou X, et al. WNT10B functional dualism: beta-catenin/Tcf-dependent growth promotion or independent suppression with deregulated expression in cancer. Mol Biol Cell 2007;18:4292–4303.
35. Yang ZF, Ho DW, Ng MN, et al. Significance of CD90(+) cancer stem cells in human liver cancer. Cancer Cell 2008;13:153–166.
36. Dontu G, Abdallah WM, Foley JM, et al. In vitro propagation and transcriptional profiling of human mammary stem/progenitor cells. Genes Dev 2003;17:1253–1270.
37. Fang D, Nguyen TK, Leishear K, et al. A tumorigenic subpopulation with stem cell properties in melanomas. Cancer Res 2005;65:9328–9337.
38. Sato N, Meijer L, Skaltsounis L, et al. Maintenance of pluripotency in human and mouse embryonic stem cells through activation of Wnt signaling by a pharmacological GSK-3-specific inhibitor. Nat Med 2004;10:55–63.
39. Balzar M, Winter MJ, de Boer CJ, et al. The biology of the 17-1A antigen (Ep-CAM). J Mol Med 1999;77:699–712.
40. Trzpis M, McLaughlin PM, de Leij LM, et al. Epithelial cell adhesion molecule: more than a carcinoma marker and adhesion molecule. Am J Pathol 2007;171:386–395.
41. Dalerba P, Dylla SJ, Park IK, et al. Phenotypic characterization of human colorectal cancer stem cells. Proc Natl Acad Sci U S A 2007;104:10158–10163.
42. Ma S, Chan KW, Hu L, et al. Identification and characterization of tumorigenic liver cancer stem/progenitor cells. Gastroenterology 2007;132:2542–2556.
43. Yin AH, Miraglia S, Zanjani ED, et al. AC133, a novel marker for human hematopoietic stem and progenitor cells. Blood 1997;90:5002–5012.
44. Fargeas CA, Corbeil D, Huttner WB. AC133 antigen, CD133, prominin-1, prominin-2, etc.: prominin family gene products in need of a rational nomenclature. Stem Cells 2003;21:506–508.
45. Shmelkov SV, Butler JM, Hooper AT, et al. CD133 expression is not restricted to stem cells, and both CD133+ and CD133- metastatic colon cancer cells initiate tumors. J Clin Invest 2008;118:2111–2120.
46. Hill RP, Perris R. "Destemming" cancer stem cells. J Natl Cancer Inst 2007;99:1435–1440.
47. Piccirillo SG, Reynolds BA, Zanetti N, et al. Bone morphogenetic proteins inhibit the tumorigenic potential of human brain tumour-initiating cells. Nature 2006;444:761–765.
48. Munz M, Kieu C, Mack B, et al. The carcinoma-associated antigen EpCAM upregulates c-myc and induces cell proliferation. Oncogene 2004;23:5748–5758.

49. Takahashi K, Tanabe K, Ohnuki M, et al. Induction of pluripotent stem cells from adult human fibroblasts by defined factors. Cell 2007;131:861–872.
50. Chaudry MA, Sales K, Ruf P, et al. EpCAM an immunotherapeutic target for gastrointestinal malignancy: current experience and future challenges. Br J Cancer 2007;96:1013–1019.
51. Nagrath S, Sequist LV, Maheswaran S, et al. Isolation of rare circulating tumour cells in cancer patients by microchip technology. Nature 2007;450:1235–1241.

Received March 9, 2008. Accepted December 1, 2008.

Reprint requests

Address requests for reprints to: Xin Wei Wang, PhD, Liver Carcinogenesis Section, Laboratory of Human Carcinogenesis, Center for Cancer Research, National Cancer Institute, 37 Convent Drive, Building 37, Room 3044A, MSC 4258, Bethesda, Maryland 20892-4258. e-mail: xw3u@nih.gov; fax: (301) 496-0497.

Acknowledgments

Microarray data are available publicly at http://www.ncbi.nlm.nih.gov/geo/ (accession number: GSE5975).

The authors thank Drs Curtis Harris and Sharon Pine for critical readings of the manuscript; Ms Barbara Taylor and Dr Susan Garfield for technical assistance; Drs Ali Brivanlou (Rockefeller University), Steve Strom (University of Pittsburgh), and Bert Vogelstein (Johns Hopkins University) for generously providing their research materials.

Conflicts of interest

The authors disclose no conflicts.

Funding

The authors disclose the following: This work was supported in part by the Intramural Research Program of the Center for Cancer Research, the US National Cancer Institute. Dr Yang, Dr HY Wang, Dr Jia, Dr Ye, Dr Qin, and Dr Tang were supported by research grants from the China National Natural Science Foundation for Distinguished Young Scholars (30325041) and the China National "863" R&D High-Tech Key Project (2002BA711A02-4). Dr Reid was supported by a sponsored research grant from Vesta Therapeutics (Research Triangle Park, NC), National Institutes of Health grants (RO1 AA014243 and RO1 IP30-DK065933), and a US Department of Energy grant (DE-FG02-02ER-63477). Sponsors had no role in the study design, data collection, analysis, and interpretation. Dr Yamashita, Dr Ji, Dr Budhu, Dr Forgues, Dr Yang, Dr Wang, Dr Jia, Dr Ye, Dr Wauthier, Dr Minato, Dr Honda, Dr Kaneko, and Dr Wang disclose no conflicts.

Common Transcriptional Signature of Tumor-Infiltrating Mononuclear Inflammatory Cells and Peripheral Blood Mononuclear Cells in Hepatocellular Carcinoma Patients

Yoshio Sakai, Masao Honda, Haruo Fujinaga, Isamu Tatsumi, Eishiro Mizukoshi, Yasunari Nakamoto, and Shuichi Kaneko

Department of Gastroenterology, Kanazawa University, School of Medicine, Kanazawa, Japan

Abstract

Hepatocellular carcinoma (HCC) is frequently associated with infiltrating mononuclear inflammatory cells. We performed laser capture microdissection of HCC-infiltrating and noncancerous liver-infiltrating mononuclear inflammatory cells in patients with chronic hepatitis C (CH-C) and examined gene expression profiles. HCC-infiltrating mononuclear inflammatory cells had an expression profile distinct from noncancerous liver-infiltrating mononuclear inflammatory cells; they differed with regard to genes involved in biological processes, such as antigen presentation, ubiquitin-proteasomal proteolysis, and responses to hypoxia and oxidative stress. Immunohistochemical analysis and gene expression databases suggested that the up-regulated genes involved macrophages and Th1 and Th2 CD4 cells. We next examined the gene expression profile of peripheral blood mononuclear cells (PBMC) obtained from CH-C patients with or without HCC. The expression profiles of PBMCs from patients with HCC differed significantly from those of patients without HCC ($P < 0.0005$). Many of the up-regulated genes in HCC-infiltrating mononuclear inflammatory cells were also differentially expressed by PBMCs of HCC patients. Analysis of the commonly up-regulated or down-regulated genes in HCC-infiltrating mononuclear inflammatory cells and PBMCs of HCC patients showed networks of nucleophosmin, SMAD3, and proliferating cell nuclear antigen that are involved with redox status, the cell cycle, and the proteasome system, along with immunologic genes, suggesting regulation of anticancer immunity. Thus, exploring the gene expression profile of PBMCs may be a surrogate approach for the assessment of local HCC-infiltrating mononuclear inflammatory cells. [Cancer Res 2008;68(24):10267–79]

Introduction

Hepatocellular carcinoma (HCC) is one of the most frequent malignancies worldwide (1). It commonly develops from chronic liver diseases, such as viral hepatitis (2) and chronic hepatitis, resulting from hepatitis C virus (HCV) infection, is a major risk factor. Indeed, 7% of patients with liver cirrhosis (LC) caused by persistent HCV (LC-C) infection develop HCC annually (3).

Cancer tissues are often associated with infiltrating inflammatory cells, such as tumor-associated macrophages (4), T lymphocytes (5), and antigen-presenting cells (6). These tumor-infiltrating mononuclear inflammatory cells are thought to be important modulators of HCC (7). However, their actual role remains controversial. Increased numbers in HCC have been correlated with a fair prognosis (8), but tumor-infiltrating mononuclear inflammatory cells in HCC tissues have also been found to involve more FOXP3$^+$ regulatory T cells (9) and provide a cancer-favorable environment that leads to resistance to therapy. Characterization of tumor-infiltrating mononuclear inflammatory cells may be valuable in understanding tumor immunology and, possibly, in predicting the prognosis of HCC patients (7).

Peripheral blood mononuclear cells (PBMCs) consist of immune cells, such as monocytes and lymphocytes, and are essential players in the host immune defense system, which responds to various abnormal conditions in the host (10). PBMCs and tumor-infiltrating mononuclear inflammatory cells contain CTLs, specifically cytocidal to cancer tissues (11) and regulatory T cells that can suppress the host immune response against cancer (9). Thus, PBMCs may potentially reflect host immune status. However, there are limited assays for assessing the immune status of PBMCs, such as a proliferation assay, measurements of cytokine production, and the assessment of cytocidal potential.

The advent of cDNA microarray technology for the analysis of gene expression profiles has been useful in comprehensively disclosing underlying molecular features and has provided considerable information for basic science and clinical medicine. We have analyzed gene expression in liver diseases (12, 13) and believe it may become a useful diagnostic tool using liver tissue biopsy samples (14). We have also reported that gene expression profiling of PBMCs predicted the effect of IFN for the eradication of HCV (15) and can provide biomarkers not only for the control of blood sugar but also possibly for predisposing diabetic factors (16). Gene expression profiling of PBMCs from patients with renal cell carcinoma can be used to predict their response to systemic chemotherapy (17). Thus, gene expression information from the cellular components of peripheral blood may be useful in interpreting the internal condition of the patient.

In this study, we used DNA microarray technology to examine differences in gene expression profiles between HCC-infiltrating and noncancerous liver-infiltrating mononuclear inflammatory cells, which were selectively microdissected (12), and the gene expression profiles of PBMCs from LC-C patients with or without HCC. We observed distinct transcriptional features of HCC-infiltrating mononuclear inflammatory cells, reflecting the immune status of the local environment. Intriguingly, the transcriptional features of the HCC-infiltrating mononuclear inflammatory cells were shared with PBMCs from HCC patients. Thus, we suggest the possibility that the gene expression profile of PBMCs may be useful as a clinical surrogate biomarker for the assessment of

Note: Supplementary data for this article are available at Cancer Research Online (http://cancerres.aacrjournals.org/).

Requests for reprints: Shuichi Kaneko, 13-1 Takara-machi, Kanazawa, Ishikawa 920-8641, Japan. Phone: 81-76-265-2233; Fax: 81-76-234-4250; E-mail: skaneko@m-kanazawa.jp.

doi:10.1158/0008-5472.CAN-08-0911

the internal environment of HCC patients with chronic hepatitis C (CH-C) infection.

Materials and Methods

Study subjects. All patients participating in this study had advanced chronic liver disease, cirrhosis, or persistent HCV infection. Twelve patients who developed HCC as a consequence of advanced chronic liver disease related to hepatitis C and who underwent surgical treatment were enrolled (Supplementary Table S1). HCC and noncancerous liver tissues were obtained and frozen. For analysis of gene expression profiles in PBMCs, 32 LC patients without HCC and 30 LC patients with HCC (Supplementary Table S2) were included. Development of HCC was diagnosed by computed tomography (CT) or magnetic resonance imaging with contrast reagents and abdominal angiography with CT imaging in arterial and portal flow phases (18). The pathologic tumor node metastasis classification system of the Liver Cancer Study Group of Japan was used for the staging of HCC. LC was diagnosed by pathologic findings in biopsy specimens where available; otherwise, radiological imaging, platelet counts, serum hyaluronic acid levels, and indocyanine green retention rates were considered for the diagnosis of cirrhosis. The study has been approved by the institutional review board, and informed consent was obtained from all patients enrolled in the study.

Isolation of PBMCs. PBMCs were isolated from heparinized blood samples by Ficoll-Hipaque density gradient centrifugation, as reported previously (15).

Laser capture microdissection. HCC and noncancerous liver tissues obtained during surgery were frozen in optimum cutting temperature compound (Sakura Finetech; ref. 13). All HCC tissues were nodular and clearly separated by noncancerous tissues macroscopically. Cells infiltrating HCC tissues were visualized under a microscope and precisely excised by laser capture microdissection (LCM) using a CRI-337 (Cell Robotics, Inc.), as previously performed (Supplementary Fig. S1*A*; ref. 12). Cells infiltrating noncancerous tissues of CH-C patients were visualized and excised similarly.

RNA isolation and amplification. Total RNA was isolated from PBMCs or tissue samples using a microRNA isolation kit (Stratagene) in accordance with the supplied protocol with slight modifications. Isolated RNA was then amplified twice using antisense RNA and an Amino Allyl MessageAmp aRNA kit (Ambion), as described previously (13). The reference RNA sample was isolated from the PBMCs of a 29-yr-old healthy male volunteer and was amplified in the same manner. Amplified RNAs from the PBMCs of patients and the healthy volunteer were labeled with Cy5 and Cy3 (Amersham), respectively. Equal amounts of amplified RNAs were hybridized to an oligo-DNA chip (AceGene Human Oligo Chip 30K, Hitachi Software Engineering Co., Ltd.) overnight and were then washed for image scanning.

DNA microarray image analysis. The fluorescence intensity of each spot on the oligo-DNA chip was determined using a DNA Microarray Scan Array G (PerkinElmer). The images obtained were quantified using a DNASIS array (v2.6, Hitachi Software Engineering Co., Ltd). For normalization, the intensity of each spot without oligo-DNA was subtracted from that with oligo-DNA in the same block. A validated spot was determined when the intensity of the spot was within the intensity ± 2 SDs for each block. By calibrating the median to base quantity, the intensities of all spots were adjusted for normalization between Cy5 and Cy3.

Quantitative real-time detection PCR. Real-time detection PCR (RTD-PCR) was performed as previously described (15). Briefly, template cDNA was synthesized from 1 μg of total RNA using SuperScript II RT (Invitrogen). Primer pairs for chemokine (C-C motif) receptor 1 (*Ccr1*), histone acetyltransferase 1 (*Hat1*), mitogen-activated protein kinase kinase 1 interacting protein 1 (*Map2k1ip1*), phosphatidylinositol glycan anchor biosynthesis, class B (*PigB*), toll-like receptor 2 (*Tlr2*), superoxide dismutase 2 (*Sod2*), cytokeratin 8 (*Krt8*), *Krt18*, *Krt19*, and glyceraldehydes-3-phosphate dehydrogenase, as an internal control of expression, were purchased from the TaqMan assay reagents library (Applied Biosystems). Synthesized cDNA was mixed with the TaqMan Universal Master Mix (Applied Biosystems), as well as each primer pair and reaction was performed using ABI PRISM 7900HT. Relative expression level of each gene was calculated compared with that of internal control in each sample. Results are expressed as means ± SE.

Flow cytometry analysis. Flow cytometry analysis was performed as described previously (19). Briefly, isolated PBMCs were incubated in PBS supplemented with 2% bovine serum albumin (Sigma-Aldrich JAPAN K.K.) with antihuman CCR1 and CCR2 antibodies labeled with Alexa Fluor 647 (Becton Dickinson Pharmingen). The fluorescence intensity of the cells was measured using a FACSort (Becton Dickinson).

Immunohistochemistry. Surgically obtained HCC and noncancerous liver tissues were fixed with neutral buffered formalin, embedded in paraffin, cut into 4-μm sections, and mounted on microscope slides. The fixed slides were deparaffinized and subjected to heat-induced epitope retrieval 98°C for 40 min. After blocking endogenous peroxidase activity in the tissue specimen using 3% hydrogen peroxide, the slides were incubated with appropriately diluted primary antibodies, antihuman CD4 or anti-human CD14 mouse monoclonal antibodies (Visionbiosystems Novocastra). The reaction was visualized by the REAL EnVision Detection System (DAKO) followed by counterstaining with hematoxylin.

Statistical analysis. Hierarchical clustering and principal component analysis of gene expression was performed using BRB-ArrayTools.[1] Fisher's exact test was used to examine the significance of hierarchical clustering in the dendrogram. A class prediction was performed by three nearest neighbors, incorporating genes that were differentially expressed at the $P = 0.002$ significance level, as assessed by the random variance t test (BRB-ArrayTools). For genes to analyze in a pathway, we used a P value of <0.05 with 2,000 permutations to avoid underestimating the presence of meaningful signaling pathways that were coordinately up-regulated or down-regulated with subtle differences (13). The cross-validated misclassification rate was computed, and at least 2,000 permutations were performed for a valid permutation P value. The univariate t values for comparing the classes were used as weights. Student's t-test was performed for RTD-PCR data, and P values of <0.05 were deemed to be statistically significant. The population of CCR1-positive or CCR2-positive cells in PBMCs by flow cytometry analysis was tested for differences (with $P < 0.05$) by the Mann-Whitney U-test, using SPSS software (SPSS Japan, Inc.).

Analysis of expression data for biological processes and networks. As for genes significantly up-regulated or down-regulated in HCC-infiltrating mononuclear inflammatory cells compared with noncancerous liver-infiltrating mononuclear inflammatory cells or in PBMCs in LC without HCC compared with LC with HCC at $P < 0.05$, we have performed analysis of the biological processes using the MetaCore software suite (GeneGo), as described previously (13). Possible networks were created according to the list of the differentially expressed genes using the MetaCore database, a unique curated database of human protein-protein and protein-DNA interactions, transcription factors, and signaling, metabolic, and bioactive molecules. The P value was calculated as described previously (13).

Gene expression data of major leukocyte types and analysis of DNA microarray expression data. Gene expression data for leukocytes were retrieved through publicly accessible databases.[2] The gene set database GDS1775, which includes gene expression data for major leukocyte types, was obtained and subjected to one-way clustering analysis using BRB-Array Tools with genes that were up-regulated in HCC-infiltrating mononuclear inflammatory cells for the enrolled cases above.

Results

Gene expression in mononuclear inflammatory cells infiltrating into HCC tissue. HCC is frequently associated with infiltrating mononuclear inflammatory cells (20), and various attempts have been made to understand their biological significance

[1] http://linus.nci.nih.gov/BRB-ArrayTools.html
[2] http://www.ncbi.nlm.nih.gov/geo/

(8, 9, 21). We selectively obtained HCC-infiltrating mononuclear inflammatory cells by LCM and compared their gene expression profiles with those of noncancerous liver-infiltrating mononuclear inflammatory cells obtained in the same way (Supplementary Fig. S1*A*; Supplementary Table S1). The gene expression profiles of HCC-infiltrating mononuclear inflammatory cells showed that 115, 206, and 773 genes were up-regulated and 52, 114, and 750 genes were down-regulated compared with those of noncancerous liver-infiltrating mononuclear inflammatory cells at P levels of <0.005, <0.01, and <0.05, respectively (Geo accession no.[3] GSE 10461; Supplementary Fig. S1*B*).

Genes at the $P < 0.05$ level were analyzed with regard to their role in biological processes in HCC-infiltrating mononuclear inflammatory cells compared with noncancerous liver-infiltrating mononuclear inflammatory cells using the MetaCore pathway analysis software. The significant processes, in which the up-regulated genes in HCC-infiltrating mononuclear inflammatory cells were involved, included antigen presentation, an immunologically important process in antigen-presenting cells, such as monocyte/macrophages and dendritic cells (Table 1; ref. 22). The genes involved in this process were the genes for the CD1d molecule and C-type lectin domain family 4 for glycolipid antigen recognition (23, 24) and CD86, an accessory molecule indispensable for provoking an immune response (25), suggesting an activated immune reaction in these cells. The up-regulated genes in HCC-infiltrating mononuclear inflammatory cells were also involved in the ubiquitin-proteasomal proteolysis process, with significant genes, such as those encoding ubiquitin-conjugating enzymes and proteasome subunits. This process is required to eradicate unnecessary proteins, which are ubiquitinated, and then degraded in proteasomes (26). Processes related to the steps of gene expression, such as transcription by RNA polymerase II, mRNA processing, and the process of the cell cycle were also represented in the genes up-regulated in HCC-infiltrating mononuclear inflammatory cells, indicating enhanced cellular activity. Genes involved in the process of double-strand breaks, such as topoisomerase II α4 (27), and proliferating cell nuclear antigen (PCNA; ref. 28) genes involved in responses to hypoxia and oxidative stress, such as thioredoxin, peroxiredoxin, and antioxidant protein, were also up-regulated, suggesting that HCC-infiltrating mononuclear inflammatory cells were in an activated inflammatory status and under hypoxic or oxidative stress, presumably caused by the HCC. Thus, the profile of up-regulated genes in HCC-infiltrating mononuclear inflammatory cells suggested an inflammatory status, possibly triggered by antigenic stimulation of HCC tissues.

Fewer processes were identified for the down-regulated genes. One intriguing process identified was that of integrin-mediated cell matrix adhesion, suggesting that HCC-infiltrating mononuclear inflammatory cells may be less adhesive in the local tissues where they were found (Supplementary Table S3).

Subpopulation analysis of HCC-infiltrating mononuclear inflammatory cells using immunohistochemistry and transcriptional analysis. Tumor-infiltrating mononuclear inflammatory cells consist of a mixed cell population, including macrophages, effector T cells, and regulatory T cells, which have been considered to be both cancer-favorable or cancer-unfavorable (8, 21). HCC-infiltrating and noncancerous liver-infiltrating mononuclear inflammatory cells were immunohistochemically evaluated to examine the characteristics of the subpopulations. CD14-positive monocytes/macrophages were prominent in HCC-infiltrating mononuclear inflammatory cells, whereas they were rarely observed in noncancerous liver-infiltrating mononuclear inflammatory cells (Fig. 1*A*). CD4-positive helper T cells were observed in both HCC tissues and noncancerous liver tissues, although in noncancerous liver tissues, these cells tended to accumulate within the aggregates of mononuclear inflammatory cells, whereas they seemed to be scattered in HCC-infiltrating mononuclear inflammatory cells (Fig. 1*A*).

Next, we examined the genes that were significantly up-regulated in HCC-infiltrating mononuclear inflammatory cells compared with noncancerous liver-infiltrating mononuclear inflammatory cells, relative to subpopulations of leukocytes, and explored how they may be relevant to leukocyte subpopulations, using the database of the human immune cell transcriptome in the Gene Expression Omnibus[3] (Geo accession no. GDS1775), which covers 26 immune regulatory cells, such as T cells, B cells, natural killer cells, macrophages, dendritic cells, basophils, and eosinophils. Among the 206 extracted, up-regulated genes in HCC-infiltrating mononuclear inflammatory cells (at the $P < 0.01$ level), 97 annotated genes were used for one-way hierarchical clusters (Fig. 1*B*). Most genes among 97 annotated up-regulated genes in HCC-infiltrating mononuclear inflammatory cells were shown to be expressed with higher magnitude in lipopolysaccharide-stimulated or lipopolysaccharide-unstimulated macrophages than in other types of major leukocytes. The next subpopulations, including the second most number of genes for relatively high magnitude of expression, were Th1 and Th2 CD4 cells under conditions supplemented with interleukin-12 (IL-12) and IL-4, respectively (Geo accession no.[3] GSM90858), secreting Th1 and Th2 cytokine profiles, respectively, suggesting that featured genes expressed in HCC-infiltrating mononuclear inflammatory cells were indicative of CD4 helper T cells, secreting a variety of cytokines.

Thus, this expression analysis showed that, in HCC lesions with tumor antigens, there was an accumulation of antigen-presenting cells, monocyte/macrophages, and CD4 helper T cells, which were in a cytokine-secreting condition, with enhanced cellular biological activities, including ubiquitin-proteasomal proteolysis, presumably under a hypoxic and oxidative stress environment caused by the HCC. The overall inflammatory status represented by HCC-infiltrating mononuclear inflammatory cells was not determined in terms of an anticancer effect, because no obvious shift of CD4 helper T cells to the Th1 or Th2 condition was indicated.

Distinct gene expression profile of PBMCs obtained from patients with cirrhotic liver disease complicated with HCC. The HCC-infiltrating mononuclear inflammatory cells were distinct in terms of expressed genes. The putative biological processes involving these up-regulated genes in tumor-infiltrating mononuclear inflammatory cells suggested a general influence of the HCC on the local environment of the host, represented by stress-response genes. We, thus, examined whether PBMCs in the systemic circulation of the patient might also be influenced by the development of HCC. PBMCs were obtained from 30 patients with LC associated with HCC and from 32 patients with LC not associated with HCC, and the gene expression profiles were compared (Geo accession no.[3] GSE10459).

Unsupervised hierarchical clustering analysis using 17,903 filtered genes, the expression values of which were not missing in >50% of the cases, identified two major clusters of patients, with and without HCC (data not shown). To examine the reproducibility and the reliability of the clustering, we excluded

Table 1. Biological processes for genes up-regulated in HCC-infiltrating mononuclear inflammatory cells

Biological process	−log(*P*)	Gene	ID	*t* (*T/†NT)	*P*	Cellular components‡
Antigen presentation	8.526	CD163	NM_004244	3.96	0.001	M
		CD86 antigen	NM_006889	3.28	0.006	M
		IFN, α-inducible protein 6	NM_022872	2.99	0.031	M
		IFN, γ-inducible protein 30	NM_006332	2.89	0.011	M
		Fc fragment of IgG, high affinity Ia, receptor (CD64)	NM_000566	2.85	0.013	M
		C-type lectin domain family 4, member M	NM_014257	2.73	0.020	
		CD63	NM_001780	2.51	0.024	M
		CD1D antigen	NM_001766	2.19	0.049	
Ubiqutin-proteasomeal proteolysis	6.555	Nucleoporin 107 kDa	NM_020401	4.32	0.001	
		Proteasome subunit, β type, 5	NM_002797	3.80	0.002	T, M
		Ubiquitin-conjugating enzyme E2R 2	NM_017811	3.67	0.004	
		Proteasome subunit, α type, 5	NM_002790	3.64	0.003	
		Prostaglandin E synthase 3	NM_006601	3.53	0.003	
		Ubiquitin-conjugating enzyme E2 binding protein, 1	NM_005744	2.94	0.011	
		Ubiquitin-conjugating enzyme E2E 3	NM_006357	2.75	0.017	
		DnaJ (Hsp40) homologue, subfamily A, member 1	NM_001539	2.47	0.028	
		Syntaxin 5	BC012137	2.19	0.046	
ER and cytoplasm	5.704	Chaperonin containing TCP1, subunit 8 (θ)	NM_006585	3.71	0.002	T, M
		Peptidylprolyl isomerase A	NM_021130	3.69	0.002	
		ERO1-like	NM_014584	3.03	0.009	T, M
		Peptidylprolyl isomerase C	BC002678	2.68	0.017	M
		SEC63 homologue	AF119883	2.59	0.020	
		Peptidylprolyl isomerase B	NM_000942	2.54	0.023	
		Chaperonin containing TCP1, subunit 4 (δ)	NM_006430	2.53	0.023	
		FK506 binding protein 3, 25 kDa	NM_002013	2.46	0.026	T, M
		Heat shock 70 kDa protein 5	AF188611	2.45	0.027	
mRNA processing	5.143	Small nuclear ribonucleoprotein polypeptide B	NM_003092	4.65	0.000	
		Small nuclear ribonucleoprotein polypeptide F	BC002505	3.28	0.005	T
		DEAD (Asp-Glu-Ala-Asp) box polypeptide 20	NM_007204	3.22	0.006	
		Cleavage and polyadenylation specific factor 6	NM_007007	3.16	0.010	
		Cleavage stimulation factor subunit 2	NM_001325	3.10	0.008	T
		Heterogeneous nuclear ribonucleoprotein A2/B1	NM_031243	2.94	0.010	
		PRP4 pre-mRNA processing factor 4 homologue B	NM_003913	2.90	0.020	
		Gem-associated protein 4	NM_015721	2.64	0.019	T
		LSM6 homologue	NM_007080	2.63	0.019	
		Exportin 1	NM_003400	2.42	0.029	
		RNA-binding motif protein 8A	AF127761	2.41	0.030	
		Splicing factor, arginine/serine-rich 1	M72709	2.39	0.036	
Transcription by RNA polymerase II	4.298	TAF9 RNA polymerase II	NM_016283	5.01	0.001	
		General transcription factor IIH, polypeptide 3, 34 kDa	NM_001516	4.74	0.001	
		TAF6-like RNA polymerase II	NM_006473	3.91	0.002	
		Nuclear receptor corepressor 1	AF044209	3.64	0.007	
		TATA box binding protein	NM_003194	2.89	0.018	

(*Continued on the following page*)

Table 1. Biological processes for genes up-regulated in HCC-infiltrating mononuclear inflammatory cells (Cont'd)

Biological process	−log(*P*)	Gene	ID	*t* (*T/† NT)	*P*	Cellular components‡
		Cofactor required for Sp1 transcriptional activation	NM_004270	2.82	0.014	T, M
		SUB1 homologue	NM_006713	2.59	0.021	
		General transcription factor II, I	NM_033001	2.55	0.023	T, M
		GCN5-like 2	NM_021078	2.34	0.048	
		TBP-like 1	NM_004865	2.24	0.043	
Double-strand breaks repair	3.289	RAD51 homologue C	NM_058216	5.24	0.000	T
		Werner syndrome	AF091214	4.99	0.000	T
		NIMA-related kinase 1	AK027580	3.27	0.007	
		Protein phosphatase 2	AF086924	3.24	0.023	
		Protein phosphatase 6	NM_002721	3.13	0.007	
		Proliferating cell nuclear antigen	NM_002592	2.80	0.014	T
		Topoisomerase II α-4	AF285159	2.57	0.033	T
ESR1-nuclear pathway	2.886	Nuclear receptor corepressor 1	AF044209	3.64	0.007	
		Nuclear receptor coactivator 4	X77548	3.19	0.007	
		Dopachrome tautomerase	NM_001922	3.04	0.019	
		COP9, subunit 5	NM_006837	2.77	0.014	
		Tissue specific extinguisher 1	NM_002734	2.70	0.018	M
		SCAN domain containing 1	NM_033630	2.50	0.026	
		Kinase insert domain receptor	NM_002253	2.35	0.047	
Cell cycle	2.241	Cyclin-dependent kinase inhibitor 3	NM_005192	4.60	0.000	
		Erythrocyte membrane protein band 4.1	NM_004437	3.47	0.014	
		RAN, member RAS oncogene family	NM_006325	3.38	0.004	T
		Cyclin C	NM_005190	3.14	0.008	
		Cell division cycle 42	NM_044472	3.14	0.007	
		Cyclin-dependent kinase-like 1	NM_004196	2.77	0.033	
		Cell division cycle 73	NM_024529	2.72	0.043	M
		Cell division cycle 27	NM_001256	2.57	0.043	
		Microtubule-actin cross-linking factor 1	AK023285	2.57	0.025	
		Histone cluster 1	NM_005323	2.30	0.047	
		Cyclin-dependent kinase 7	NM_001799	2.13	0.050	
		Cyclin G_2	NM_004354	2.48	0.038	
Response to hypoxia and oxidative stress	1.401	Thioredoxin	NM_003329	2.64	0.019	T, M
		Glutaredoxin 2	NM_016066	2.63	0.024	T, M
		Peroxiredoxin 3	NM_006793	2.81	0.016	T, M
		Peroxiredoxin 2	NM_005809	2.27	0.039	
		Antioxidant protein 2	NM_004905	2.22	0.042	
		Peroxiredoxin 1	NM_002574	2.21	0.043	T, M
		Microsomal glutathione *S*-transferase 2	NM_002413	2.41	0.031	M

*T represents tumor-infiltrating mononuclear inflammatory cells.
†NT represents non–tumor-infiltrating mononuclear inflammatory cells.
‡Cellular components predominantly expressed cellular components among 26 immune regulatory cells (T, Th cells; M, macrophage).

unchanged genes in all samples (genes with less than a 1.8-fold difference in >85% of samples) to remove noise. This hierarchical clustering analysis using 1,917 filtered genes confirmed two clear clusters in patients with or without HCC (Fig. 2*A*). In one major cluster, including the most LC cases, there was a subcluster, LC/HCC, which included more of the HCC patients located next to the cluster of patients with HCC (LC/HCC; Fig. 2*A*). The reproducibility of the clustering (proportion, averaged over replications and over all pairs of samples in the same cluster, BRB-ArrayTools) was 93%. Sensitivity and specificity to HCC in this cluster analysis is 88% and 76%, respectively. These cirrhotic patients without HCC were followed for at least a further 12 months to detect HCC; none of those in the LC group developed HCC over this time. The principal component analysis was performed with the filtered 1,917 genes and the two major groups; classifying LC and HCC were similarly observed (Fig. 2*B*).

To further confirm that gene expression in the PBMCs of patients with HCC was distinct from that in patients without HCC, analysis of PBMC gene expression was performed by a

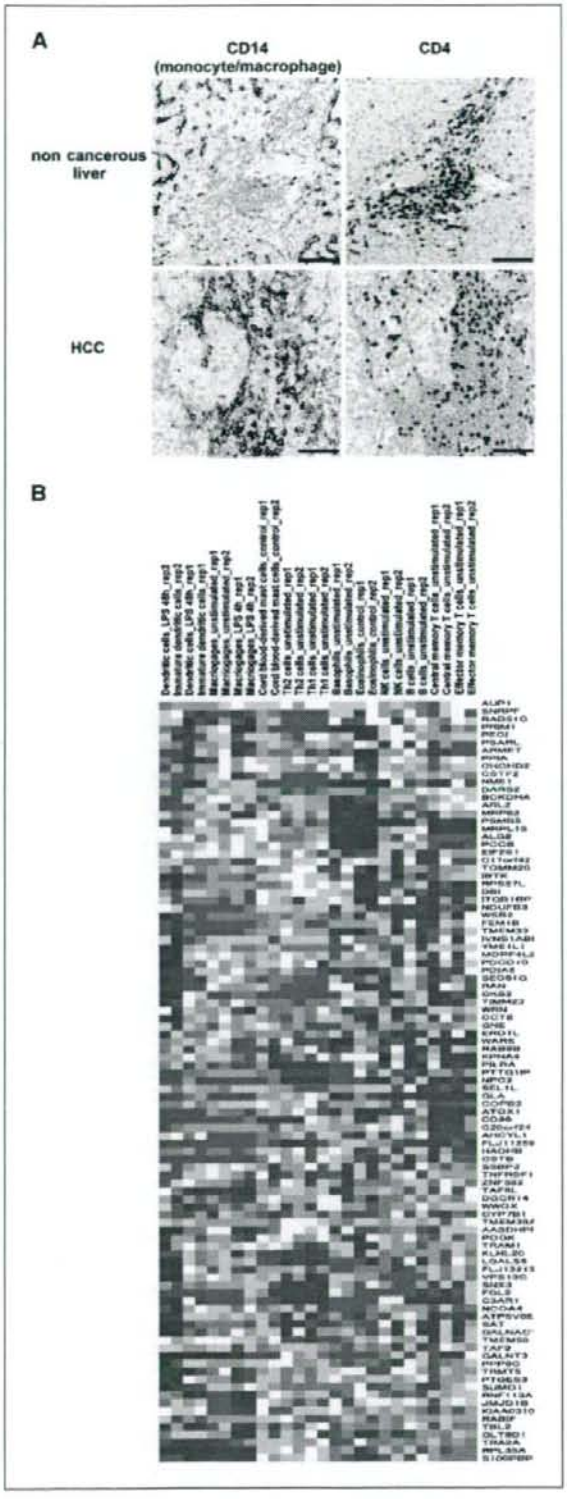

supervised learning method using categories of LC-C or HCC, age, gender, serum alanine aminotransferase (ALT), and α-fetoprotein (AFP). It showed that patients with or without HCC were significant classifiers ($P < 0.0005$), assigned with 1,430 predictor genes ($P < 0.002$; Table 2). Of 32 patients with LC, eight (25%) were misclassified as having HCC, and 2 of 30 patients with HCC (6.7%) were misclassified as not having HCC, indicating that the overall accuracy of the prediction of a patient with or without HCC was 84% (Table 2). Other clinical variables supposed to be related to HCC occurrence, such as age (ref. 29; >68 or ≤ 68 years old), gender (30), and ALT(ref. 31; >50 or ≤50 IU/L), could not differentiate gene expression in PBMCs. AFP (>20 or ≤20 ng/mL) was actually significant but was a much less powerful classifier ($P < 0.02$, assigned with 301 classifier genes). The prediction accuracy for categories of LC-C versus HCC and the AFP value >20 versus ≤20 ng/mL is not significantly affected whenever the number of predictor genes is reduced to below 62 (Supplementary Fig. S2). Taken together, these results by unsupervised and supervised analysis methods indicate that HCC development in LC-C patients significantly affects the gene expression profile in PBMCs.

Features of biological processes for which gene expression was significantly altered in PBMCs in HCC patients. We next examined the biological processes possibly affected by HCC development, given the expression profiles in PBMCs from patients with HCC. Statistical analysis showed that 867 genes were up-regulated and 989 genes were down-regulated in PBMCs from patients with HCC, compared with those without HCC ($P < 0.005$). Six representative genes, *Ccr1, Hat, Map2k1ip1, PigB, Tlr2,* and *Sod2,* were randomly selected from genes which were biologically important and differentially expressed between LC and HCC groups, and their expression was confirmed by RTD-PCR (Supplementary Fig. S3*A*). To exclude the possibility of circulating cancer cells, we have also examined the expression of *Afp, Krt8, Krt18,* and *Krt19*. No expression was detected for *Afp* (data not shown), and no statistically significant difference was found for expression of *Krt8, Krt18,* and *Krt19* between patients with HCC and without HCC (Supplementary Fig. S3*A*). The expression data were also confirmed by flow cytometric analysis. We evaluated how many cells in blood expressed CCR1 and CCR2 and confirmed that populations expressing CCR1 and CCR2 were significantly higher in PBMCs from patients with HCC than those without (Supplementary Fig. S3*B*). To understand the biological processes in PBMCs for which up-regulated or

Figure 1. HCC-infiltrating mononuclear inflammatory cells involve monocyte/macrophage and helper T cell. *A*, immunohistochemical staining. Many of the HCC-infiltrating mononuclear inflammatory cells expressed monocyte/macrophage marker, CD14. In contrast, few CD14-positive cells were seen in noncancerous liver-infiltrating mononuclear inflammatory cells. *Bars*, 100 μm. *B*, one-way hierarchical clustering analysis of gene expression of immune-mediating cells with genes whose expression was up-regulated in HCC-infiltrating mononuclear inflammatory cells. Data for gene expression in immune-mediating cells were retrieved from Gene Expression Omnibus[2] (Geo accession no. GDS 1775). By excluding genes missing from over half of the immune-mediating cells, 206 genes up-regulated in HCC-infiltrating mononuclear inflammatory cells were filtered, and the remaining 97 genes were used for clustering. Transverse and longitudinal titles show the type of immune-mediating cell and gene symbols, respectively. Color indicates relative expression magnitude of 97 up-regulated genes HCC-infiltrating mononuclear inflammatory cells among retrieved expression data of major leukocyte types deposited in the public database. The red and blue color means relatively high or low magnitude of expression among 26 retrieved expression data of leukocytes. The heat-map shows that helper T cells and unstimulated or stimulated macrophages included more blocks with the red color.

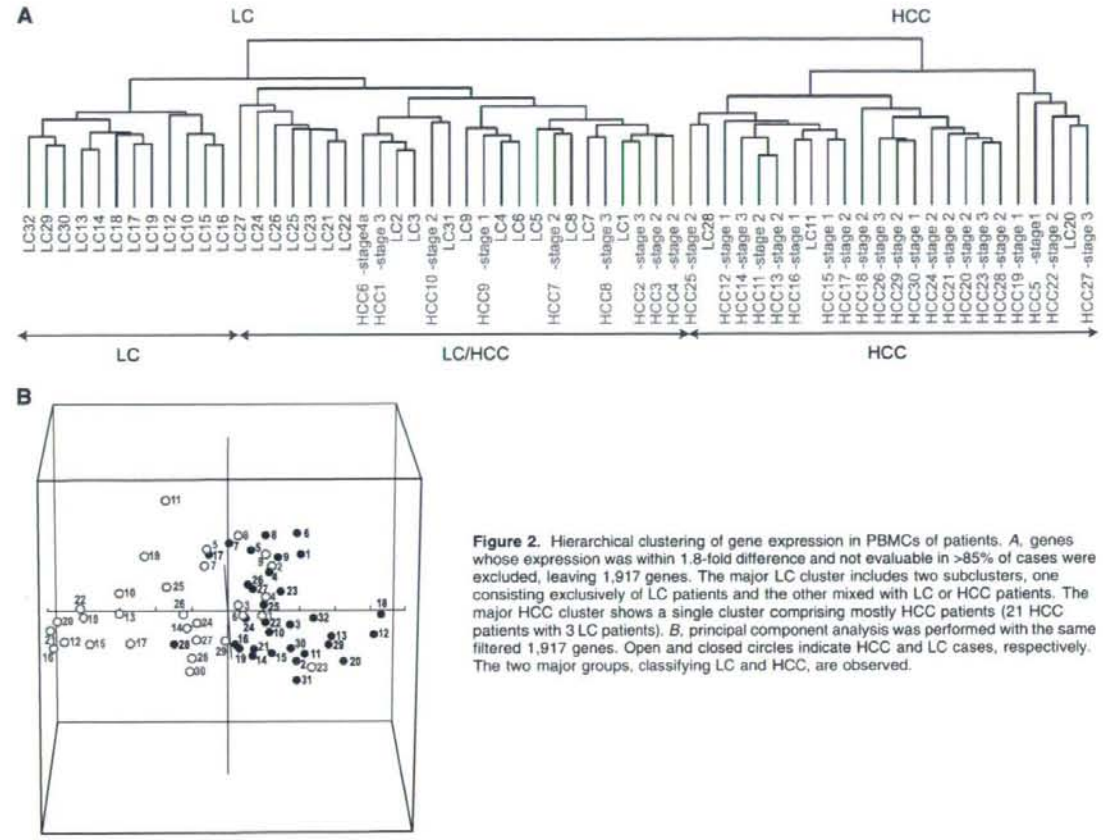

Figure 2. Hierarchical clustering of gene expression in PBMCs of patients. *A*, genes whose expression was within 1.8-fold difference and not evaluable in >85% of cases were excluded, leaving 1,917 genes. The major LC cluster includes two subclusters, one consisting exclusively of LC patients and the other mixed with LC or HCC patients. The major HCC cluster shows a single cluster comprising mostly HCC patients (21 HCC patients with 3 LC patients). *B*, principal component analysis was performed with the same filtered 1,917 genes. Open and closed circles indicate HCC and LC cases, respectively. The two major groups, classifying LC and HCC, are observed.

down-regulated genes were observed, we used MetaCore. The up-regulated genes in PBMCs from patients with HCC were involved in processes such as ubiquitin-proteasomal proteolysis (e.g., heat shock 70 kDa protein 4, ubiquitin conjugating enzymes), mRNA processing (e.g., heterogeneous nuclear ribonucleoproteins, RNA methyltransferase), antigen presentation (e.g., MHC class I polypeptide-related sequence A, B), cell cycle (e.g., HAT1, PCNA), and the response to hypoxia and oxidative stress (e.g., glutaredoxin 2, SOD2, thioredoxin; Table 3). These differentially up-regulated biological processes were also up-regulated processes in HCC-infiltrating inflammatory cells (Table 1). Thus, PBMCs from HCC patients present antigens in conditions of hypoxia and oxidative stress. Additionally, genes involved in other processes, such as apoptosis (e.g., apoptotic peptidase activating factor 1,

Table 2. Supervised learning methods for gene expression of PBMCs

Classifier category	Clinical groups	Total no. cases	No. cases misclassified	Classifier *P* values	No. genes in the classifiers ($P < 0.002$)
LC-C versus HCC	LC-C	32	8	<0.0005	1,430
	HCC	30	2		
Age (y)	>68	31	12	0.317	32
	≦68	31	16		
Gender	Male	25	15	0.178	20
	Female	37	9		
ALT (IU/L)	>50	26	20	0.82	28
	≦50	36	14		
AFP (ng/mL)	>20	29	10	0.02	301
	≦20	33	10		

Table 3. Biological processes for genes up-regulated in PBMCs of HCC patients

Biological process	−log(*P*)	Gene	ID	*t* (T/NT)	*P*	Cellular components
Ubiquitin-proteasomal proteolysis and ER	22.237	Ubiquitin specific peptidase 8	D29956	5.54	0.0000	
		Protein phosphatase 3 (formerly 2B),	NM_000945	4.90	0.0000	
		Heat shock transcription factor 2	NM_004506	4.52	0.0000	
		Heat shock 90 kDa protein 1	NM_005348	4.45	0.0000	T, M
		Ubiquitin protein ligase E3A	NM_000462	4.27	0.0001	
		Ubiquitin-conjugating enzyme E2D1	NM_003338	3.62	0.0006	M
		Phosphatidylinositol glycan, class B	NM_004855	3.57	0.0007	
		Ubiquitin-conjugating enzyme E2D2	NM_003339	3.49	0.0009	
		Ubiquitin-conjugating enzyme E2D3	NM_003340	3.18	0.0023	
		RAN binding protein 2	NM_006267	3.11	0.0029	
		Ubiquitin-conjugating enzyme E2A	NM_003336	3.09	0.0030	
		Activating transcription factor 6	NM_007348	3.03	0.0037	T, M
		Ubiquitin specific protease 7	NM_003470	2.92	0.0050	
		Heat shock 70 kDa protein 9B	NM_001746	2.91	0.0050	
		T-complex 1	NM_030752	2.76	0.0077	
		Glutaredoxin 2	NM_016066	2.70	0.0093	
		Ubiquitin-conjugating enzyme E2N	NM_003348	2.68	0.0096	
		Ubiquitin-conjugating enzyme E2 variant 2	AF049140	2.66	0.0110	
		Ubiquitin specific protease 14	NM_005151	2.20	0.0322	
		Progesterone receptor-associated p48 protein	NM_003932	2.16	0.0353	
		Heat shock 70 kDa protein 4	AB023420	2.16	0.0346	
		Ubiquitin-conjugating enzyme E2L 3	NM_003347	2.14	0.0363	
		Tenascin XB	NM_004381	2.13	0.0377	
		Ubiquitin specific peptidase 33	AB029020	2.12	0.0385	M
mRNA processing	20.087	Heterogeneous nuclear ribonucleoprotein R	NM_005826	3.90	0.0003	T
		RNA (guanine-7-) methyltransferase	NM_003799	3.29	0.0024	
		Heterogeneous nuclear ribonucleoprotein D-like	NM_031372	3.23	0.0020	
		Survival motor neuron domain containing 1	NM_005871	3.12	0.0031	
		Ribonueclease, rnase a family, 4	NM_002937	2.93	0.0052	
		Heterogeneous nuclear ribonucleoprotein A1	NM_002136	2.68	0.0094	
		Heterogeneous nuclear ribonucleoprotein K	NM_002140	2.46	0.0170	
		Heterogeneous nuclear ribonucleoprotein U	NM_031844	2.36	0.0216	
		UPF3, yeast, homologue of, A	NM_023011	2.35	0.0228	
		Alternative splicing factor	M72709	2.03	0.0471	
Antigen presentation	10.124	Janus kinase 1	NM_002227	3.38	0.0013	
		MHC, class II, DO α	NM_002119	3.09	0.0031	
		MHC, class II, DR α	NM_019111	2.67	0.0098	
		MHC class I polypeptide-related sequence B	NM_005931	2.60	0.0122	
		MHC class I polypeptide-related sequence A	NM_000247	2.26	0.0276	
		Tumor necrosis factor receptor–associated factor 6	NM_004620	2.05	0.0456	
Cell Cycle	6.185	Karyopherin (importin) β 2	NM_002270	4.32	0.0001	
		Histone acetyltransferase 1	NM_003642	4.15	0.0001	T, M
		V-myc myelocytomatosis viral oncogene homologue	NM_002467	3.57	0.0008	
		Transforming, acidic coiled-coil containing protein 1	NM_006283	3.38	0.0014	

(*Continued on the following page*)

Table 3. Biological processes for genes up-regulated in PBMCs of HCC patients (Cont'd)

Biological process	−log(*P*)	Gene	ID	*t* (T/NT)	*P*	Cellular components
		Centromere protein B, 80 kDa	X05299	3.37	0.0014	
		Conductin	AF078165	3.07	0.0032	
		Amyloid β precursor protein-binding protein 1	NM_003905	2.99	0.0040	T
		Centromere protein C 1	NM_001812	2.90	0.0054	
		Heterochromatin-like protein 1	BC000954	2.72	0.0085	
		Mature T-cell proliferation 1	BC002600	2.49	0.0154	
		Proliferating cell nuclear antigen	NM_002592	2.46	0.0166	
		CSE1 chromosome segregation 1-like	NM_001316	2.42	0.0186	M
		Karyopherin α4 (importin α3)	NM_002268	2.37	0.0209	
		Signal transducers and activators of transcription–like protein	BC010854	2.36	0.0214	
		M-phase phosphoprotein 6	NM_005792	2.34	0.0228	
		Extra spindle pole bodies homologue 1	NM_012291	2.20	0.0316	
Apoptosis	4.811	Cathepsin S	NM_004079	5.59	0.0000	M
		YME1-like 1	NM_014263	5.49	0.0000	T, M
		Cullin 5	NM_003478	4.65	0.0000	M
		Apoptotic peptidase activating factor 1	NM_001160	3.53	0.0008	
		Cullin 2	NM_003591	3.43	0.0012	M
		Amyloid β precursor protein-binding protein 1	NM_003905	2.99	0.0040	T
		Caspase 9	NM_032996	2.96	0.0044	
		F-box only protein 5	NM_012177	2.88	0.0055	
		Cullin 1	NM_003592	2.52	0.0146	
		Caspase 4	NM_001225	2.23	0.0293	
		Caspase 1	NM_033293	2.02	0.0475	
TCR signaling and immune related	5.462	Protein tyrosine phosphatase, receptor type, C	NM_002838	5.72	0.0000	
		Phosphoinositide-3-kinase, catalytic, α polypeptide	NM_006218	5.38	0.0000	
		Activating transcription factor 2	NM_001880	3.98	0.0002	
		Chemokine (c-c motif) receptor 1	NM_001295	3.90	0.0003	
		NCK adaptor protein 1	NM_006153	3.18	0.0024	
		Chemokine (c-c motif) receptor 2	NM_000647	2.78	0.0075	
		Toll-like receptor2	NM_003264	2.75	0.0078	
		Inositol 1,4,5-triphosphate receptor, type 1	NM_002222	2.24	0.0290	
		T-cell receptor α-chain	X01403	2.05	0.0452	
Response to hypoxia and oxidative stress	2.655	MAP2K1IP1	NM_021970	6.51	0.0000	
		Glutathione s-transferase θ 2	NM_000854	3.43	0.0011	
		Hypoxia-inducible factor 1, α subunit	NM_001530	2.99	0.0040	
		MAP/ERK kinase kinase 5	NM_005923	2.73	0.0086	
		Glutaredoxin 2	NM_016066	2.70	0.0093	
		Peroxiredoxin 3	NM_006793	2.68	0.0157	
		Catalase	NM_001752	2.50	0.0151	
		Plasma glutathione peroxidase 3 precursor	NM_002084	2.19	0.0329	
		Superoxide dismutase 2	NM_000636	2.10	0.0400	
		Thioredoxin	NM_003329	2.05	0.0186	

caspase 9) and T-cell receptor (TCR) signaling (e.g., CCR1, CCR2, TCR α-chain), were also up-regulated in PBMCs from patients with HCC, suggesting vulnerabilities of PBMCs and activated T-cell signaling, respectively, in HCC development.

Biological processes involving the down-regulated genes in PBMCs from patients with HCC included skeletal muscle development, the estrogen receptor 1 (ESR1) nuclear pathway, NOTCH signaling, feeding, and neurohormones signaling, neurogenesis, leptin signaling, and IL-12, IL-15, and IL-18 signaling (Supplementary Table S4), showing no obvious connection compared with the down-regulated genes in HCC-infiltrating mononuclear inflammatory cells (Supplementary Table S3). These results indicate that HCC development in cirrhotic liver can influence PBMCs, providing distinct transcriptional features of up-regulated genes even during the operable stage of HCCs.

Networks of genes commonly up-regulated or down-regulated in both PBMCs and HCC-infiltrating mononuclear inflammatory cells. Analysis of the gene expression profiles of HCC-infiltrating mononuclear inflammatory cells and PBMCs from HCC patients showed that the development of HCC altered the gene expression of local infiltrating mononuclear inflammatory cells and systemically circulating PBMCs; interestingly, the affected biological processes were largely the same. To further explore these presumed local and systemic influences resulting from HCC development, we examined how individual genes were affected by constructing a network.

We found 773 up-regulated and 750 down-regulated significant genes in HCC-infiltrating mononuclear inflammatory cells compared with noncancerous liver-infiltrating mononuclear inflammatory cells at the $P < 0.05$ level. In PBMC gene expression, we observed 2,111 up-regulated and 2,027 down-regulated genes in the PBMCs of HCC patients, compared with LC patients at the $P < 0.05$ level. Among these genes, 378 were significant in both HCC-infiltrating mononuclear inflammatory cells and PBMCs from patients with HCC (Fig. 3*A*). For these 378 genes commonly altered genes, 70% of them were up-regulated or down-regulated in both HCC-infiltrating mononuclear inflammatory cells and PBMCs from HCC patients, whereas expression of the remaining 30% of them was discordant.

We used MetaCore software to perform network construction for 172 up-regulated and 93 down-regulated genes in both HCC-infiltrating mononuclear inflammatory cells and PBMCs from HCC patients. The signal pathway network revealed three central genes, PCNA (32), SMAD3 (33), and nucleophosmin (34), which were all up-regulated in HCC-infiltrating mononuclear inflammatory cells and PBMCs from HCC patients (Fig. 3*B*). PCNA had interactions with proteasome subunit genes, PSMC2, PSMC6, PSMD12, and thioredoxin and DNA polymerase iota genes. SMAD3 was linked with cyclin-dependent kinase 7 and cyclin G_2 with various genes related to the cell cycle. Nucleophosmin was connected to ubiquitin-conjugating enzyme e2e3 and glutaredoxins. Notably, FOXP3, a marker of regulatory T cells, and Janus-activated kinase 3 (JAK3), related to interleukin signaling (35), were up-regulated and down-regulated, respectively, in HCC-infiltrating mononuclear inflammatory cells and PBMCs from HCC patients in the constructed gene network.

The network constructed for individual genes whose expression was commonly altered in HCC-infiltrating mononuclear inflammatory cells and PBMCs from HCC patients also supported a condition of HCC-related stress. The network also indicated that immune reactions in patients with HCC are complex, because down-regulated JAK3, an interleukin signaling molecule, and up-regulated FOXP3 and SMAD3, known molecules of anticancer immunity, are involved in this network. Biological processes in HCC-infiltrating mononuclear inflammatory cells and PBMCs from HCC patients also included the antigen-presentation process.

Discussion

In this study, we explored gene expression in local infiltrating mononuclear inflammatory cells in HCC and noncancerous liver tissues and in PBMCs obtained from patients with hepatitis C–related LC, with or without HCC. Gene expression profiles of HCC-infiltrating mononuclear inflammatory cells were quite distinct from those of noncancerous liver-infiltrating mononuclear inflammatory cells, showing their differing roles in anticancer immunity. We also investigated gene expression in systemically circulating PBMCs from LC-C patients with or without HCC and found that PBMC gene expression profiles from patients with or without HCC were significantly different. Intriguingly, many biological processes involving the up-regulated genes were shared between HCC-infiltrating mononuclear inflammatory cells and PBMCs from HCC patients, suggesting that the local inflammatory effect evoked by HCC development is systemically projected in the host.

Tumor-infiltrating mononuclear inflammatory cells have been investigated to examine their roles in local cancer tissues. We have selectively obtained aggregates of infiltrating mononuclear inflammatory cells in HCC and noncancerous liver tissues by LCM without contamination of carcinoma or parenchymal cells. We have shown that the process of antigen-presentation (36) is a distinguishing feature for up-regulated genes in HCC-infiltrating mononuclear inflammatory cells compared with noncancerous liver-infiltrating mononuclear inflammatory cells. Consistently, immunohistochemical staining of HCC and noncancerous liver tissues revealed that the HCC-infiltrating mononuclear inflammatory cells are primarily monocytes/macrophages, a lineage of phagocytes and antigen-presenting cells (37). Helper CD4 T cells were also found but seemed to be scattered in the HCC-infiltrating mononuclear inflammatory cells, compared with their intensive accumulation in infiltrating mononuclear inflammatory cells in noncancerous liver tissues. Correspondingly, analysis using a publicly available gene expression database of major leukocytes showed that up-regulated genes in HCC-infiltrating mononuclear inflammatory cells were primarily featured for macrophages and Th1 and Th2 CD4 cells, preconditioned with IL-12 and IL-4, respectively. These findings could be interpreted in that HCC expresses tumor-antigens (38) different from the surrounding noncancerous liver tissues; consequently, phagocytes gather in HCC tissues, take up antigens expressed by HCC tissues, and interact with CD4 cells (39). The scattered distribution and transcriptional features of both the Th1 and Th2 predisposed status of CD4 helper T cells in HCC-infiltrating mononuclear inflammatory cells suggests their versatile inflammatory status in cancer immunity, although there was no obvious shift of the Th1/Th2 balance, which is considered to be important in cancer immunity (40).

Other characteristic biological processes involving the up-regulated genes in HCC-infiltrating mononuclear inflammatory cells included the response to hypoxia and oxidative stress (41), the ubiquitin-proteasome system, cell cycle, mRNA processing, ER, and cytoplasm. The ubiquitin-proteasome system is unique to eukaryotic cells and important in maintaining the normal biological activity of cells, with pleiotropic effects in higher animals (42). The cell cycle requires precise regulation of cyclin-dependent kinase under strict control by ubiquitination and subsequent protein degradation (32). Taken together, these processes involving the up-regulated genes may reflect a protective local response of the host, corresponding to the stress environment of HCC. In this sense, the double-strand break repair gene up-regulation may be interpreted as the cells responding to maintain normal cellular activities although they are exposed to a harmful environment by the HCC (43).

The biological processes involving the up-regulated genes in PBMCs from HCC patients, compared with those from LC-C patients without HCC, were, to a substantial degree, the same, involving the up-regulated genes in HCC-infiltrating mononuclear

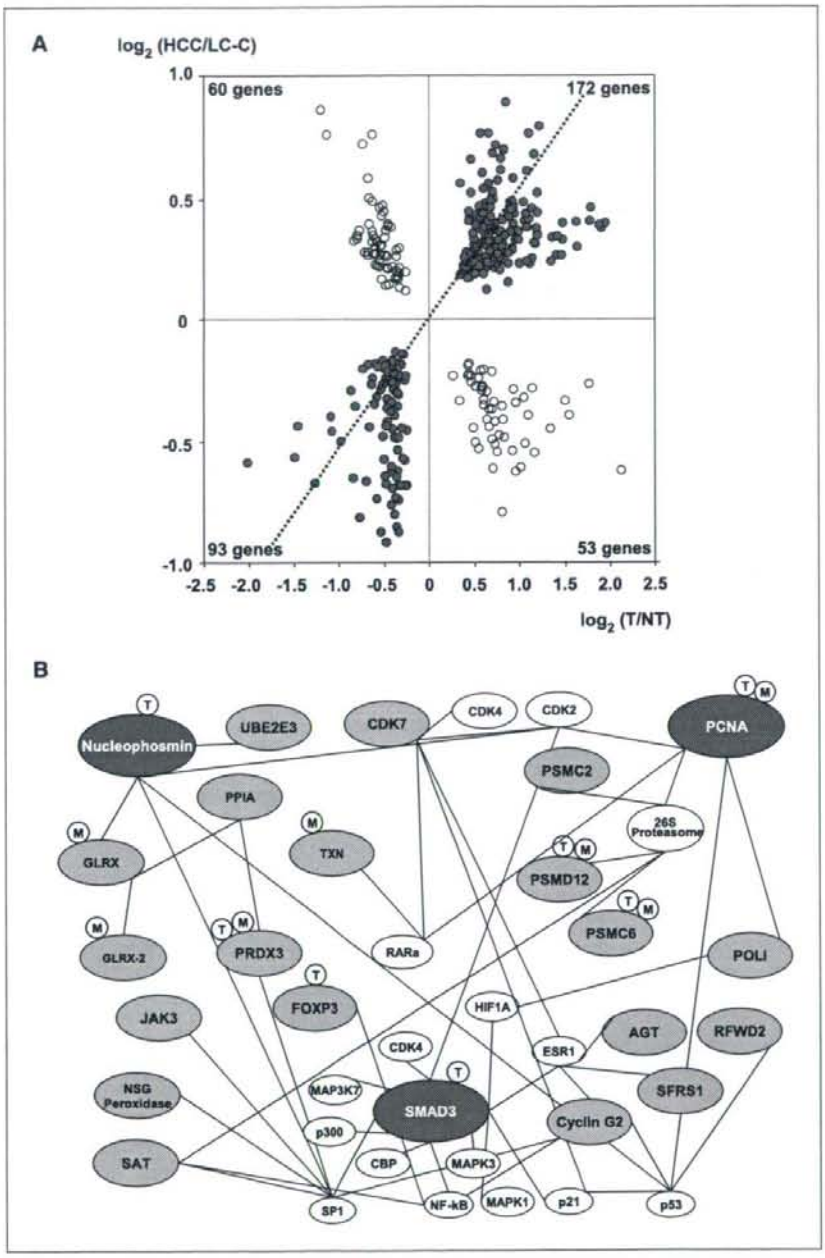

Figure 3. Features of commonly affected genes in PBMCs of HCC patients and HCC-infiltrating mononuclear inflammatory cells. *A*, scatter plots of gene expression ratios between local infiltrating mononuclear inflammatory cells and PBMCs. The axes show the binary logarithm value of the gene expression ratio of HCC-infiltrating mononuclear inflammatory cells over noncancerous liver-infiltrating mononuclear inflammatory cells on the *x* axis and the ratio of PBMCs from HCC patients over LC-C patients on the *y* axis. The right top quadrant includes 172 genes whose expression was up-regulated in HCC-infiltrating mononuclear inflammatory cells and in PBMCs from HCC patients, whereas the left bottom quadrant includes 93 genes down-regulated in both. *B*, interactive network for differentially expressed genes between PBMCs of HCC and LC-C patients and between infiltrating cells adjacent to HCC and noncancerous liver tissues. The three highlighted genes are PCNA, SMAD3, and nucleophosmin, which are related to the redox system, ubiquitin-proteasome system, and cell cycle, in addition to some immunologic gene connections. T or M at each node represent T lymphocytes or monocytes, respectively, and indicate the cell population in which each gene was expressed. The red-filled and blue-filled circles indicate up-regulation or down-regulation, respectively, in HCC-infiltrating mononuclear inflammatory cells and PBMCs from HCC patients.

inflammatory cells, such as ubiquitin-proteasomal proteolysis, ER, and cytoplasm, mRNA processing, antigen presentation, the cell cycle, and the response to hypoxia and oxidative stress. The reflection of these transcriptional features of HCC-infiltrating mononuclear inflammatory cells by PBMCs from HCC patients suggests a systemically projected influence of local HCC development, which is presumably the result of the stress environment caused by HCC and the host's reaction even when the size of the tumor is relatively small. In addition to exploring these biological processes, we also constructed networks of individual genes, the expression of which was similarly up-regulated or down-regulated, to depict commonly affected biological processes in tumor-infiltrating mononuclear inflammatory cells and PBMCs under HCC development in more detail. The networks highlighted three central genes, nucelophosmin, PCNA, and SMAD3, as up-regulated genes. They are connected to individual genes involved in ubiquitin,

proteasomes, the cell cycle, and oxidative stress (Fig. 3*B*). Interestingly, the immunologically important molecules, FOXP3 and JAK3, are in the network as up-regulated and down-regulated genes, respectively. FOXP3 is a transcriptional marker for regulatory T cells (44), and SMAD3 is also believed to be important in maintaining regulatory T cells (45). JAK3, which is associated with the interleukin receptor common γ chain (35) and is important in lymphoid development (46), was also involved in the network, suggesting that HCC influences the host immune system, which can be observed not only in HCC-infiltrating mononuclear inflammatory cells but also in the PBMCs of HCC patients. Thus, the network features of individual genes, commonly affected in HCC-infiltrating mononuclear inflammatory cells and PBMCs from HCC patients, further imply that the anticancer immunity of the host in response to HCC development involves the antigen presentation process to initiate the immune reaction.

The mechanism by which PBMCs from HCC patients reflect the transcriptional features of HCC-infiltrating mononuclear inflammatory cells requires further study. We observed that the population of CCR1-expressing and CCR2-expressing cells in PBMCs from HCC patients was higher than in those from LC-C patients. However, HCC-infiltrating mononuclear inflammatory cells did not show up-regulation of these genes. The meaning of the up-regulated CCR1 and CCR2 should be further investigated because chemokines are key molecules for the recruitment of inflammatory cells, regulating cellular adhesion and transendothelial migration, and the activation of inflammatory cells (47). The biological process of integrin-mediated cell matrix adhesion, genes involved in which were down-regulated in HCC-infiltrating mononuclear inflammatory cells, may suggest that these cells were able to remigrate into the microcirculation with the enriched blood flow in HCC tissues. The process of integrin-mediated cell matrix adhesion in HCC-infiltrating inflammatory cells may imply weaker adhesion of infiltrating mononuclear inflammatory cells to cancer tissues compared with noncancerous liver tissues (48). PBMCs are also presumed to be affected by humoral factors from HCC tissues (49). Another possibility is the presence of hematogenous spreading and circulating HCC cells because mRNA for AFP was detected in circulation (50). Because two-thirds of HCC patients enrolled for gene expression analysis of PBMCs showed serum AFP value <100, the presence of circulating HCC cells would not be evaluated by the detection of *Afp* gene expression alone. Therefore, we have examined expression of *Krt8*, *Krt18*, and *Krt19*, as well as *Afp*. Despite of the possibility of circulating cancer cells, we neither detected expression of *Afp* nor found significantly different expression of *Krt8*, *Krt18*, and *Krt19* between HCC and LC-C patients without HCC. Furthermore, genes up-regulated in HCC tissues compared with noncancerous liver tissues[3] did not correlate to up-regulated genes in PBMCs of HCC patients, indicating that different signature of gene expression in PBMCs between HCC and LC-C patients is not the reflection of the possible migrating cells from HCC tissues. In addition, all HCC cases, except for a case in gene expression analysis of PBMCs, were radiologically free of tumor thrombus in the vessel, which was indicative of microscopic invasion free or concomitant with invasion in the periphery of third or lower branch of vessels, suggesting that contribution of circulating cancer cells were presumed to be sufficiently small for the distinct difference of gene expression signature of PBMCs.

Although the number of enrolled HCC patients for analysis with local inflammatory cells was relatively small compared with the number of patients for analysis of PBMCs, our study has shown shared features of gene expression profiles of HCC-infiltrating mononuclear inflammatory cells and PBMCs from HCC patients, showing a complex immune status of the host in anticancer immunity. This finding suggests the possibility that readily accessible PBMCs can be used as a surrogate tissue to assess the local inflammatory environment surrounding cancers through examination of gene expression profiles.

Disclosure of Potential Conflicts of Interest

No potential conflicts of interest were disclosed.

Acknowledgments

Received 3/10/2008; revised 9/5/2008; accepted 9/25/2008.

The costs of publication of this article were defrayed in part by the payment of page charges. This article must therefore be hereby marked *advertisement* in accordance with 18 U.S.C. Section 1734 solely to indicate this fact.

We thank Nakamura for her invaluable contribution to this study.

[3] Unpublished data.

References

1. El-Serag HB, Mason AC. Rising incidence of hepatocellular carcinoma in the United States. N Engl J Med 1999;340:745–50.
2. Motola-Kuba D, Zamora-Valdes D, Uribe M, Mendez-Sanchez N. Hepatocellular carcinoma. An overview. Ann Hepatol 2006;5:16–24.
3. Yoshida H, Shiratori Y, Moriyama M, et al. Interferon therapy reduces the risk for hepatocellular carcinoma: national surveillance program of cirrhotic and noncirrhotic patients with chronic hepatitis C in Japan. IHIT Study Group. Inhibition of Hepatocarcinogenesis by Interferon Therapy. Ann Intern Med 1999;131:174–81.
4. Farinati F, Marino D, De Giorgio M, et al. Diagnostic and prognostic role of α-fetoprotein in hepatocellular carcinoma: both or neither? Am J Gastroenterol 2006; 101:524–32.
5. Yu P, Lee Y, Liu W, et al. Priming of naive T cells inside tumors leads to eradication of established tumors. Nat Immunol 2004;5:141–9.
6. Preynat-Seauve O, Schuler P, Contassot E, Beermann F, Huard B, French LE. Tumor-infiltrating dendritic cells are potent antigen-presenting cells able to activate T cells and mediate tumor rejection. J Immunol 2006;176: 61–7.
7. Kawata A, Une Y, Hosokawa M, Uchino J, Kobayashi H. Tumor-infiltrating lymphocytes and prognosis of hepatocellular carcinoma. Jpn J Clin Oncol 1992;22:256–63.
8. Hirano S, Iwashita Y, Sasaki A, Kai S, Ohta M, Kitano S. Increased mRNA expression of chemokines in hepatocellular carcinoma with tumor-infiltrating lymphocytes. J Gastroenterol Hepatol 2007;22:690–6.
9. Kobayashi N, Hiraoka N, Yamagami W, et al. FOXP3+ regulatory T cells affect the development and progression of hepatocarcinogenesis. Clin Cancer Res 2007;13: 902–11.
10. Williams MA, Newland AC, Kelsey SM. The potential for monocyte-mediated immunotherapy during infection and malignancy: Part I. Apoptosis induction and cytotoxic mechanisms. Leuk Lymphoma 1999;34:1–23.
11. Nakao M, Sata M, Saitsu H, et al. CD4+ hepatic cancer-specific cytotoxic T lymphocytes in patients with hepatocellular carcinoma. Cell Immunol 1997;177: 176–81.
12. Honda M, Kawai H, Shirota Y, Yamashita T, Kaneko S. Differential gene expression profiles in stage I primary biliary cirrhosis. Am J Gastroenterol 2005;100:2019–30.
13. Honda M, Yamashita T, Ueda T, Takatori H, Nishino R, Kaneko S. Different signaling pathways in the livers of patients with chronic hepatitis B or chronic hepatitis C. Hepatology 2006;44:1122–38.
14. Daiba A, Inaba N, Ando S, et al. A low-density cDNA microarray with a unique reference RNA: pattern recognition analysis for IFN efficacy prediction to HCV as a model. Biochem Biophys Res Commun 2004;315:1088–96.
15. Tateno M, Honda M, Kawamura T, Honda H, Kaneko S. Expression profiling of peripheral-blood mononuclear cells from patients with chronic hepatitis C undergoing interferon therapy. J Infect Dis 2007;195:255–67.
16. Takamura T, Honda M, Sakai Y, et al. Gene expression profiles in peripheral blood mononuclear cells reflect the pathophysiology of type 2 diabetes. Biochem Biophys Res Commun 2007;361:379–84.
17. Burczynski ME, Twine NC, Dukart G, et al. Transcriptional profiles in peripheral blood mononuclear cells prognostic of clinical outcomes in patients with advanced renal cell carcinoma. Clin Cancer Res 2005;11: 1181–9.

18. Matsui O. Imaging of multistep human hepatocarcinogenesis by CT during intra-arterial contrast injection. Intervirology 2004;47:271–6.
19. Sakai Y, Morrison BJ, Burke JD, et al. Vaccination by genetically modified dendritic cells expressing a truncated neu oncogene prevents development of breast cancer in transgenic mice. Cancer Res 2004;64:8022–8.
20. Wada Y, Nakashima O, Kutami R, Yamamoto O, Kojiro M. Clinicopathological study on hepatocellular carcinoma with lymphocytic infiltration. Hepatology 1998;27:407–14.
21. Fu J, Xu D, Liu Z, et al. Increased regulatory T cells correlate with CD8 T-cell impairment and poor survival in hepatocellular carcinoma patients. Gastroenterology 2007;132:2328–39.
22. Xu W, Roos A, Daha MR, van Kooten C. Dendritic cell and macrophage subsets in the handling of dying cells. Immunobiology 2006;211:567–75.
23. Gadola SD, Dulphy N, Salio M, Cerundolo V. Vα24-JαQ-independent, CD1d-restricted recognition of α-galactosylceramide by human CD4(+) and CD8α(β(+) T lymphocytes. J Immunol 2002;168:5514–20.
24. Feinberg H, Taylor ME, Weis WI. Scavenger receptor C-type lectin binds to the leukocyte cell surface glycan Lewis(x) by a novel mechanism. J Biol Chem 2007;282:17250–8.
25. Orabona C, Grohmann U, Belladonna ML, et al. CD28 induces immunostimulatory signals in dendritic cells via CD80 and CD86. Nat Immunol 2004;5:1134–42.
26. Demartino GN, Gillette TG. Proteasomes: machines for all reasons. Cell 2007;129:659–62.
27. Petruti-Mot AS, Earnshaw WC. Two differentially spliced forms of topoisomerase IIα and β mRNAs are conserved between birds and humans. Gene 2000;258:183–92.
28. Naryzhny SN, Desouza LV, Siu KW, Lee H. Characterization of the human proliferating cell nuclear antigen physico-chemical properties: aspects of double trimer stability. Biochem Cell Biol 2006;84:669–76.
29. Velazquez RF, Rodriguez M, Navascues CA, et al. Prospective analysis of risk factors for hepatocellular carcinoma in patients with liver cirrhosis. Hepatology 2003;37:520–7.
30. Ikeda K, Arase Y, Saitoh S, et al. Prediction model of hepatocarcinogenesis for patients with hepatitis C virus-related cirrhosis. Validation with internal and external cohorts. J Hepatol 2006;44:1089–97.
31. Tarao K, Rino Y, Ohkawa S, et al. Close association between high serum alanine aminotransferase levels and multicentric hepatocarcinogenesis in patients with hepatitis C virus-associated cirrhosis. Cancer 2002;94:1787–95.
32. Cayrol C, Ducommun B. Interaction with cyclin-dependent kinases and PCNA modulates proteasome-dependent degradation of p21. Oncogene 1998;17:2437–44.
33. Riggins GJ, Thiagalingam S, Rozenblum E, et al. Mad-related genes in the human. Nat Genet 1996;13:347–9.
34. Dhar SK, Lynn BC, Daosukho C, St Clair DK. Identification of nucleophosmin as an NF-κB co-activator for the induction of the human SOD2 gene. J Biol Chem 2004;279:28209–19.
35. Oakes SA, Candotti F, Johnston JA, et al. Signaling via IL-2 and IL-4 in JAK3-deficient severe combined immunodeficiency lymphocytes: JAK3-dependent and independent pathways. Immunity 1996;5:605–15.
36. Smyth MJ, Godfrey DI, Trapani JA. A fresh look at tumor immunosurveillance and immunotherapy. Nat Immunol 2001;2:293–9.
37. Dobrovolskaia MA, Vogel SN. Toll receptors, CD14, and macrophage activation and deactivation by LPS. Microbes Infect 2002;4:903–14.
38. Kim JW, Ye Q, Forgues M, et al. Cancer-associated molecular signature in the tissue samples of patients with cirrhosis. Hepatology 2004;39:518–27.
39. Itano AA, Jenkins MK. Antigen presentation to naive CD4 T cells in the lymph node. Nat Immunol 2003;4:733–9.
40. Budhu A, Wang XW. The role of cytokines in hepatocellular carcinoma. J Leukoc Biol 2006;80:1197–213.
41. Gerald D, Berra E, Frapart YM, et al. JunD reduces tumor angiogenesis by protecting cells from oxidative stress. Cell 2004;118:781–94.
42. Pickart CM. Back to the future with ubiquitin. Cell 2004;116:181–90.
43. Liu L, Simon MC. Regulation of transcription and translation by hypoxia. Cancer Biol Ther 2004;3:492–7.
44. Ramsdell F. Foxp3 and natural regulatory T cells: key to a cell lineage? Immunity 2003;19:165–8.
45. Fantini MC, Becker C, Monteleone G, Pallone F, Galle PR, Neurath MF. Cutting edge: TGF-β induces a regulatory phenotype in CD4+CD25- T cells through Foxp3 induction and down-regulation of Smad7. J Immunol 2004;172:5149–53.
46. Park SY, Saijo K, Takahashi T, et al. Developmental defects of lymphoid cells in Jak3 kinase-deficient mice. Immunity 1995;3:771–82.
47. Baggiolini M. Chemokines and leukocyte traffic. Nature 1998;392:565–8.
48. Leon MP, Bassendine MF, Gibbs P, Thick M, Kirby JA. Immunogenicity of biliary epithelium: study of the adhesive interaction with lymphocytes. Gastroenterology 1997;112:968–77.
49. Cao M, Cabrera R, Xu Y, et al. Hepatocellular carcinoma cell supernatants increase expansion and function of CD4(+)CD25(+) regulatory T cells. Lab Invest 2007;87:582–90.
50. Wong IH, Yeo W, Leung T, Lau WY, Johnson PJ. Circulating tumor cell mRNAs in peripheral blood from hepatocellular carcinoma patients under radiotherapy, surgical resection or chemotherapy: a quantitative evaluation. Cancer Lett 2001;167:183–91.

Protein J (2008) 27:409–419
DOI 10.1007/s10930-007-9123-y

Comparative Analysis of Proteome and Transcriptome in Human Hepatocellular Carcinoma using 2D-DIGE and SAGE

Hirotaka Minagawa · Taro Yamashita · Masao Honda · Yo Tabuse · Kenichi Kamijo · Akira Tsugita · Shuichi Kaneko

Published online: 2 December 2008

Abstract Proteome analysis of human hepatocellular carcinoma was conducted using two-dimensional difference gel electrophoresis, and the protein expression profiles were compared to the mRNA expression profiles made from serial analysis of gene expression (SAGE) in identical samples from a single patient. Image-to-image analysis of protein abundances together with protein identification by peptide mass fingerprinting yielded the protein expression profiles. A total of 188 proteins were identified, and the expression profiles of 164 proteins which had the corresponding SAGE data were compared to the mRNA expression profiles. Among them, 40 proteins showed significant differences in the mRNA expression levels between non HCC and HCC. We compared expression changes of proteins with those of mRNAs. We found that the expression tendency of 24 proteins were similar to that of mRNA, whereas 16 proteins showed different or opposite tendency to the mRNA expression.

Keywords Hepatocellular carcinoma · Proteome · Two-dimensional difference gel electrophoresis · Serial analysis of gene expression

Abbreviations

HCC	Hepatocellular carcinoma
SAGE	Serial analysis of gene expression
2-DE	Two-dimensional gel electrophoresis
2D-DIGE	Two-dimensional difference gel electrophoresis
IS	Internal standard
PMSF	Phenylmethyl sulfonyl fluoride
TFA	Trifluoroacetic acid
ACN	Acetonitrile
MALDI-TOF	Matrix assisted laser desorption ionization time of flight
LC-ESI-IT	Liquid chromatography-electrospray ion trap tandem mass spectrometry
MS/MS	
PMF	Peptide mass fingerprinting

1 Introduction

Hepatocellular carcinoma (HCC) is one of the most common cancers worldwide, and a leading cause of death in Africa and Asia [16]. Although several major risks related to HCC, such as hepatitis B and/or hepatitis C virus infection, aflatoxin B1 exposure, and alcohol drinking, and genetic defects, have been revealed [11], the molecular mechanisms leading to the initiation and progression of HCC are not well-known. To find the molecular bases of hepatocarcinogenesis, comprehensive gene expression analyses have been conducted using many systems such as hepatoma cell lines [8] and tissue samples [7]. Iizuka et al. [7] reported the differential gene expression in distinct

Electronic supplementary material The online version of this article (doi:10.1007/s10930-007-9123-y) contains supplementary material, which is available to authorized users.

H. Minagawa (✉) · Y. Tabuse · K. Kamijo
Fundamental and Environmental Research Laboratories, NEC Corporation, 34 Miyukigaoka, Tsukuba, Ibaraki 305-8501, Japan
e-mail: h-minagawa@ab.jp.nec.com

T. Yamashita · M. Honda · S. Kaneko
Department of Gastroenterology, School of Medicine, Kanazawa University, Kanazawa, Japan

A. Tsugita
Proteomics Research Laboratory, Tokyo Rikakikai, Tsukuba, Japan

virologic types of HCC using oligonucleotide microarray, and they showed that 89 genes were expressed differentially between hepatitis B virus infected HCCs associated with liver cirrhosis and those not associated with liver cirrhosis.

The serial analysis of gene expression (SAGE) technique is thought to be an appropriate technique for evaluating thousands of gene expressions quantitatively, and has been used frequently to profile transcriptome [17]. We have previously done the comprehensive mRNA expression analysis in moderately differentiated HCC using SAGE. We found that many genes were expressed differentially between HCC and non HCC; INF-gamma inducible genes, superoxide dismutase 2, DEAD/H box polypeptide 5 and so on were up-regulated, whereas cytochrome P450 IIIA4 and IIA7, organic cation transporter 1 were down-regulated in HCC [22]. These genomic approaches have yielded global gene expression profiles in HCC and identified a number of candidate genes as possible biomarkers for cancer staging, prediction of prognosis, and treatment selection [13, 18]. Still, many researchers think that the proteomic study might reinforce our understanding of the molecular events accompanying HCC development because proteins rather than mRNA are the major effectors of cellular and tissue functions. It is generally accepted that mRNA and protein expression do not always correlate [4, 6], thus, protein expression analysis, which could complement the available mRNA data, is also important to understand the molecular mechanisms of HCC development.

Several proteomic researches have been performed so far on HCC using various protein separation technologies such as 2-DE followed by protein identification by mass spectrometry. The technique of two-dimensional difference gel electrophoresis (2D-DIGE), developed by Unlu et al. [21], is one of the major advances in quantitative proteomics. In 2D-DIGE, different samples pre-labeled with mass- and charge-matched fluorescent cyanine dyes, Cy3 and Cy5, are separated on the same 2D gel together with the internal standard prepared by mixing equal amounts of all samples and labeled with a third cyanine dye, Cy2. The labeled samples and internal standard are then mixed and fractionated on the same 2D gel. Coseparation of different samples on the same gel suppresses subtle changes in experimental conditions, thus enabling accurate spot detection and matching. The internal standard run on the background of all gels also facilitates gel-to-gel spot matching and allows the derivation of statistically reliable comparisons of protein abundances [1]. Recently several groups have utilized 2D-DIGE to examine protein expression changes in HCC samples [9, 10], whereas, there are few reports describing gene and protein expression profiles of the same HCC sample simultaneously [17].

We have previously analyzed gene expression changes between HCC and the adjacent non-tumor tissue extirpated from the same patient. As the patient was negative for hepatitis B and hepatitis C virus infection, we thought that the results should primarily reflect gene and protein expression changes involved in carcinogenesis. In order to complement our SAGE results, we performed proteomic research using 2D-DIGE and we compared the expression profile of proteins with that of mRNAs directly in the identical sample from a single patient.

2 Materials and Methods

2.1 HCC Sample

A 57-year-old male was admitted to the Kanazawa University Hospital and received hepatic lobectomy for treatment of a solitary HCC. The HCC sample and adjacent non-tumor liver sample were snap frozen in liquid nitrogen, and used for SAGE and 2-DE analysis. The HCC and non-tumor samples were histologically diagnosed as moderately differentiated HCC and mild hepatic fibrosis without active hepatitis, respectively. Serological tests of hepatitis B surface antigen (DAINABOT, Tokyo, Japan), hepatitis C virus antibodies (Roche Diagnostic Systems, Branchburg, NJ), and hepatitis C virus RNA by Amplicore analysis (Roche Diagnostic Systems) showed negative. Therefore, gene and protein expression change through viral infection, such as HBV [23] and HCV [3], was negligible, and the expression change together with carcinogenesis was shown clearly. All strategies used for gene expression and protein expression analysis were approved by the ethical committee of Kanazawa University Hospital.

2.2 Long SAGE

Long SAGE was performed as described previously [15]. Briefly, total RNA was purified from each homogenized tissue sample using a Totally RNA extraction kit (Ambion, Inc., Austin, TX), and polyadenylated RNA was isolated by a MicroPoly (A) Pure kit (Ambion). A total of 2.5 μg mRNA per sample was used for construction of Long SAGE libraries. Libraries were randomly sequenced at the Genomic Research Center (Shimadzu-Biotechnology, Kyoto, Japan), and the sequence files were analyzed with SAGE 2000 software. The size of each library was normalized to 300,000 transcripts per library, and the abundance of transcripts was compared by SAGE 2000 software. Monte Carlo analysis was performed to determine the statistical significance of obtaining a difference in expression in each transcript by SAGE 2000 software.

Each SAGE tag was annotated using a gene-mapping web site (http://www.ncbi.nlm.nih.gov/SAGE/index.cgi).

2.3 Protein Labeling with Cyanine Dye

Sample for 2-DE was homogenized with lysis buffer (7 M urea, 2 M thiourea, 4% w/v CHAPS, 0.8 μM aprotinin, 15 μM pepstatin, 0.1 mM PMSF, 0.5 mM EDTA, 30 mM Tris–HCl, pH 8.5) and then centrifuged at 13,000 rpm 20 min at 4 °C. The supernatants were removed and used as protein samples. The protein concentrations were determined with a protein assay reagent (Bio-Rad) according to the manufacture. The protein sample of tumor tissue was designated as HCC sample and the protein sample of noncancerous liver was designated as non HCC sample.

The experimental strategy is shown in Fig. 1. The non HCC sample (50 μg) was labeled with Cy3 dye, and the HCC sample (50 μg) was labeled with Cy5 dye. The labeled samples were combined and separated on 2-DE gels together with the internal standard (IS), which was prepared by mixing 25 μg of non HCC and HCC samples, and labeled with Cy2. Labeling reactions were carried out according to the manufacture. Each sample was labeled with 400 pmol of CyDye (GE Healthcare) on ice for 30 min in the dark and reactions were stopped by adding 1 μl of 10 mM lysine. The CyDye-labeled samples (non HCC, HCC, and IS) were mixed and left for 10 min on ice in the dark. The mixtures were added to an equal volume of the sample buffer (7 M urea, 2 M thiourea, 1% v/v IPG buffer (GE Healthcare), 2.4% v/v Destreak Reagent (GE Healthcare), 4% w/v CHAPS). Mixed samples were then adjusted to 450 μL with the rehydration buffer (7 M urea, 2 M thiourea, 0.5% v/v IPG buffer (GE Healthcare), 1.2% v/v Destreak Reagent (GE Healthcare), 4% w/v CHAPS, trace of bromophenol blue).

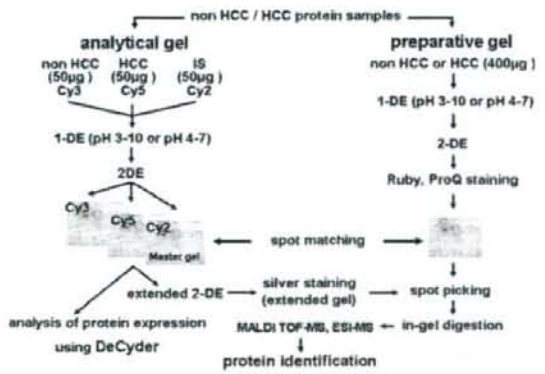

Fig. 1 Outline of 2D-DIGE analysis. After being labeled with the respective CyeDye, samples were combined with the Cy2-labeled internal standard (IS) and separated on 2-DE. The experiment was triplicate to obtain numerical; data sufficient for statistical analysis

2.4 Analytical and Preparative 2-DE for 2D DIGE Analyses

Analytical 2-DE was performed as follows: The labeled protein samples were electrophoresed in the first dimension on IPG gels (Immobiline DryStrip, GE Healthcare, pH 3–10 or pH 4–7, 24 cm) using the IPGphor system (GE Healthcare). After rehydration at 20 °C for 12 h, IEF was carried out at 500 V for 500 Vh, at 1,000 V for 1,000 Vh, and at 8,000 V for 70,000 Vh in the dark. The gel strips were equilibrated in 12 mL of the equilibration buffer A (50 mM Tris–HCl, pH 8.8, 6 M urea, 30% v/v glycerol, 2% w/v SDS, 1% w/v DTT, trace of bromophenol blue) for 15 min with gently shaking, and then were equilibrated in 12 mL of the equilibration buffer B (50 mM Tris–HCl, pH 8.8, 6 M urea, 30% v/v glycerol, 2% w/v SDS, 2.5% w/v iodoacetamide, trace of bromophenol blue) for 15 min with gently shaking. The equilibrated strips were loaded on the top of 12.5% SDS-polyacrylamide gels (24 × 20 cm) and sealed with 0.5% w/v agarose. 2D separation was performed overnight at 1 W/gel using Ettan DALTII (GE Healthcare). After 2-DE, gels were scanned with a Typhoon 9410 scanner (GE Healthcare) using filters conformable to each dye's excitation and emission wavelength, and then to analyze the high molecular region with high resolution, the scanned gels were run again at 5 W/gel for a further 16 h (extended gel). After this additional electrophoresis, the extended gels were scanned with the Typhoon scanner as described above, and then the twice-scanned gels were stained with Silver Staining Reagent (GE Healthcare) without glutaraldehyde. Samples were run in triplicate to obtain statistically reasonable results.

To obtain an adequate amount of the proteins from the individual spots for protein identification, 400 μg of the proteins extracted from the non HCC or HCC were separately run on 2-DE gels as described above. After 2-DE, these preparative gels were fixed in 10% v/v methanol and 7% v/v acetic acid aqueous solution for 30 min and stained with a fluorescent dye, SYPRO Ruby (Invitrogen) overnight at room temperature according to the manufacturer. The gels were washed twice with 10% v/v methanol and 7% v/v acetic acid for 30 min and then washed three times with distilled water for 5 min. The washed gels were scanned with the Typhoon scanner.

To detect phosphoproteins, 400 μg samples from non HCC and HCC were separately run on 2-DE gels. The gels were fixed on 50% methanol and 10% acetic acid overnight at room temperature. The gels were then washed three times, for 15 min each time with distilled water and stained

with ProQ Diamond Phosphoprotein Gel Stain (Invitrogen) for 1 h in the dark. The gels were then washed with a destaining solution (Invitrogen) three times for 30 min each time at room temperature. After obtaining the images, the ProQ Diamond-staining gels were counterstained with SYPRO Ruby to visualize the total proteins as described above.

2.5 Analysis of Gel Images

For CyDye-labeled analytical gels, a 488 nm laser and 520 nm emission filters were used for Cy2 images, a 532 nm laser and 580 nm emission filters for Cy3 images, and a 633 nm laser and 670 nm emission filters for Cy5 images. Preparative gels stained with SYPRO Ruby were scanned with a 457 nm laser and 610 nm emission filters. All gel images were obtained at 100 μm resolution and processed using ImageQuant (GE Healthcare) prior to image analysis. The analysis of gel images was performed with the DeCyder software (GE Healthcare). The Cy2, Cy3, and Cy5 images of the same gel were electrically merged and the proteins were detected as Cy3/Cy2 and Cy5/Cy2 spot pairs. For each spot pair, the normalized ratio of spot volume relative to IS (Cy3:Cy2 or Cy5:Cy2) was calculated and analyzed statistically. The statistical differences in each normalized spot volume between non HCC and HCC were analyzed by the Student's paired *t*-test using DeCyder BVA (GE Healthcare), and p value ≤ 0.05 was considered as significant changed. For protein identification by PMF, the spots visualized with SYPRO Ruby were matched to those on CyDye images.

2.6 Protein Identification

The protein spots were excised from the SYPRO Ruby stained gels using the Ettan spot picker (GE Healthcare) or manually excised from the silver stained gels. The excised protein spots collected in 96-well plates were digested in gel with porcine trypsin (Promega) using an automatic digestion robot, ProGest (Genomic Solutions), according to the manufacture. For MALDI-TOF analysis using Voyager-DE STR (Applied Biosystems), the digested and dried peptides were dissolved in 5 μL of 0.1% trifluoroacetic acid (TFA) in 50% acetonitrile (ACN). Aliquots (1 μL) were spotted on MALDI target and then 1 μL of α-cyano-4-hydroxycinnamic acid (5 mg/mL in 0.1% TFA in 60% ACN) was immediately added. MALDI-TOF analysis was carried out in reflector mode in the mass range of 850–3,000 Da. A database search was carried out against *Homo sapiens* category of NCBInr entries using MS-Fit (Protein Prospector) or ProFound (http://www.129.85.19.192/profound_bin/WebProFound.exe). The search parameters allowed for carbamidomethylation of cysteine, partial oxidation of methionine, ±0.3 Da for mass tolerance, and one missed cleavage per peptide. For LC-ESI-IT MS/MS analysis using LCQ Deca XP (Thermo Electron), the digested and dried peptide samples were dissolved in 10 μL of 0.1% TFA in 2% ACN. The samples were loaded on a C18 silica gel capillary column (Magic C18, 50 × 0.2 mm), and the elution from the column was directly connected through a sprayer to an ESI-IT MS. Mobile phase A was 2% ACN containing 0.1% formic acid, and mobile phase B was 90% ACN containing 0.1% formic acid. A linear gradient from 5% to 65% of concentration B was applied to elute peptides. The ESI-IT MS was operated in positive ion mode over the range of 350–2000 (m/z) and the database search was carried out against *Homo sapiens* category of NCBInr entries using MASCOT (Matrixscience). The identified proteins were classified according to their molecular functions and the cellular components into categories described by Gene Ontology Consortium (http://www.geneontology.org/index.shtml) using BioCompass software (NEC Corp.).

3 Results

3.1 2-DE and Protein Identification

Labeled protein samples were separated on 2-DE, and the fluorescence images were obtained (Fig. 2). In parallel to the analytical gels, samples prepared from non HCC and HCC tissues were separately run on the preparative gels for protein identification. The proteins were visualized with SYPRO Ruby, and images were directly matched to CyDye images of analytical gels. Approximately 1,100 spots were analyzed, and 361 spots representing 183 proteins were determined (Fig. 3). Three proteins were excluded from the following analysis because of ambiguous spot matching between analytical gels and preparative gels. The extended gel images mentioned in Sect. 2.4 were analyzed with DeCyder software, and about 20% of analytical spots, whose expression levels between HCC and non HCC were altered by more than 1.8-fold (230 protein spots), were selected for PMF analysis. After silver staining, these 230 spots were manually excised and 143 spots representing 66 proteins were identified. Eight proteins were newly detected in extended gels. As a result, total of 188 proteins were identified from Ruby and silver stained gels (Supplementary Table 1). The identified proteins and mRNAs were classified according to their molecular functions and the cellular components into categories described by Gene Ontology Consortium (Fig. 4a, b). As for molecular functions, about 60% of the identified proteins were classified as catalytic activity, such as metabolic enzymes, and 20% of them were classified as binding activity, such as heat shock proteins (Fig. 4a). The major cellular components of